KLOPPER, EMSIE

A STUDY ON THE PREDICTABILITY OF SEASONAL TEMPERATURE IN SOUTH AFRICA

MSc UP 1997

A STUDY ON THE PREDICTABILITY OF SEASONAL TEMPERATURE IN SOUTH AFRICA

EMSIE KLOPPER

A dissertation submitted in partial fulfilment

of the requirements for the degree

MASTER OF SCIENCE (METEOROLOGY)

in the

FACULTY OF ENGINEERING

UNIVERSITY OF PRETORIA

1997

The heavens keep telling
the wonders of God,
and the skies declare
what He has done.

Each day informs
the following day;
each night announces
to the next.

They don't speak
a word, and
there is never the
sound of a voice.

Yet their message
reaches all the earth,
and it travels
around the world.

Psalm 19:1-4

DISSERTATION SUMMARY

A STUDY ON THE PREDICTABILITY OF SEASONAL TEMPERATURE IN SOUTH AFRICA

EMSIE KLOPPER

Supervisor:	Professor J. van Heerden
Co-Supervisor:	Mr WA Landman
Department:	Civil Engineering
University:	University of Pretoria
Degree:	Master of Science (Meteorology)

Key words: Seasonal forecasting; South Africa; Sea-surface temperature; Temperature variability; Canonical correlation analysis; Singular value decomposition.

An analysis of the variability and predictability of seasonal temperature over South Africa is conducted. Possible relationships between global scale sea-surface temperature fields and seasonal temperature over South Africa are sought by means of a statistical technique namely singular value decomposition. Associations between sea-surface temperature and seasonal temperature over South Africa are evident and in particular, associations between El Niño / Southern Oscillation related signals from the oceans and seasonal temperature over the eastern half of the country. Also, a long-term warming trend in the ocean temperatures have important influences on the temperature variability over South Africa. In this study canonical correlation analysis is used to construct a forecast scheme for the prediction of seasonal temperature over South Africa at different lead times. Evolutionary patterns in the ocean temperature field are used as predictors. Categorical seasonal temperatures are predicted and evaluated for an independent test period to verify the skill and therefore usefulness of such predictions.

SAMEVATTING VAN VERHANDELING

A STUDY ON THE PREDICTABILITY OF SEASONAL TEMPERATURE IN SOUTH AFRICA

EMSIE KLOPPER

Studieleier:	Professor J. van Heerden
Mede-Studieleier:	Mnr WA Landman
Departement:	Siviele Ingenieurswese
Universiteit:	Universiteit van Pretoria
Graad:	Magister Scientiae (Weerkunde)

Sleutelwoorde: Seisoenale voorspelling; Suid-Afrika; See-oppervlak temperature; Temperatuur veranderlikheid; Kanoniese korrelasie analiese; Singuliere waarde ontleding.

'n Analiese van die veranderlikheid en voorspelbaarheid van seisoenale temperatuur in Suid-Afrika is uitgevoer. Waarskynlike verbande tussen globale skaal see-oppervlak temperature en seisoenale temperature oor Suid-Afrika is gesoek deur middel van 'n statistiese tegniek naamlik singuliere waarde ontleding. Die belangrikste verbande tussen see-oppervlak temperature en seisoenale temperature oor Suid-Afrika word geassosieer met die El Niño/Suidelike Ossilasie verskynsel. Hierdie verband is veral duidelik oor die oostelike helfte van die land. Verder word die langtermyn globale verhitting van oseane ook in verband gebring met seisoenale temperatuur oor Suid-Afrika. In hierdie studie word kanoniese korrelasie analiese gebruik om 'n voorspellingskema op te stel waarmee seisoenale temperature oor Suid-Afrika voorspel kan word vir verskillende na-yl periodes. Evolutionêre patrone in die see-oppervlak temperatuurveld word gebruik as voorspellers. Kategoriese seisoenale temperature word voorspel en geëvalueer oor 'n onafhaklike toets periode om die vaardigheid en gevolglik ook die toepasbaarheid van hierdie voorspellings te bepaal.

ACKNOWLEDGEMENTS

I wish to express my appreciation to:

- Colleague and friend, Willem Landman for his supervision and guidance
- Professor Johan van Heerden for supervising this dissertation
- Colleagues who took interest in my work, especially Gerrie Coetzee and Winifred Jordaan
- The South African Weather Bureau for using their computer facilities and data
- My husband, Riaan for his encouragement

CONTENTS

Page

LIST OF FIGURES

LIST OF TABLES

CHAPTER 1

BACKGROUND

1.1 Introduction

South Africa is a country well known for its sunshine and relatively warm, subtropical climate and although generally dry and warm, South Africa plays a major role in the economic network of southern Africa. Skilful seasonal climate predictions could benefit the economy (tourism, agriculture, industries etc.) if applied during planning and decision making processes (Madden, 1977; Preisendorfer and Mobley, 1984; Livezey and Barnston, 1988; Preisendorfer *et al.*, 1988; Palmer and Anderson, 1994). The development of skilful forecast methods has become a high priority of the South African Weather Bureau and other research organisations in southern Africa. This dissertation focuses on the predictability of seasonal surface-air temperature in South Africa.

Various factors are known to affect the continental surface-air temperature distribution on both short- and longer time scales such as height above sea level, distance from the sea, cloudiness, rainfall, advection and subsidence, to name but a few. The physical configuration and location of South Africa engender unique and extremely variable climate characteristics, both in time and space. Some of the important temperature features are discussed below.

1.2 South African Temperature Characteristics

The orography of South Africa (Figure 1.1) is known to influence the temperature distribution over the country. The escarpment forms an imposing climatic division between the high plateau (about 1250m above sea-level, reaching 3000m in the Lesotho Highlands) and the low lying coastal regions in the eastern and south-eastern side. The effect of altitude is particularly evident in the Tugela, Orange and Limpopo river valleys where temperature is higher than on the surrounding high-lying country. Generalized isotherms of mean surface temperature tend to follow these contours of the land surface with the lowest temperatures occurring along the eastern escarpment (Schulze, 1965).

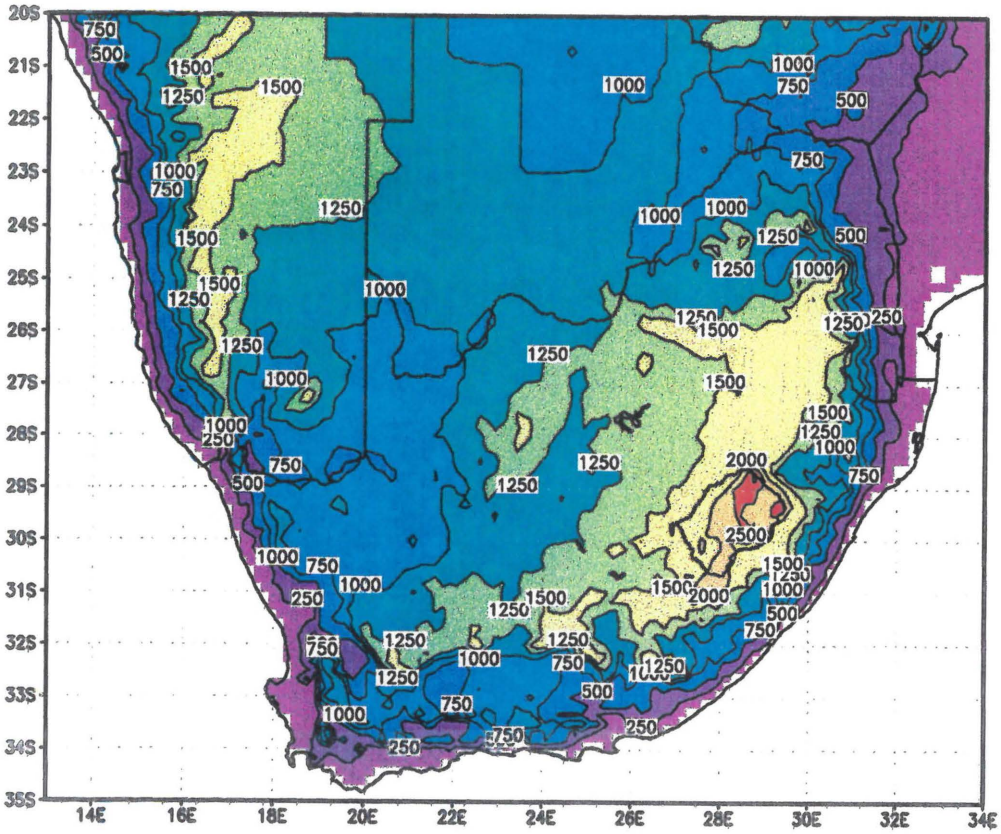

Figure 1.1 Orography of South Africa. Height in meters above sea-level

The climate of southern Africa is influenced strongly by its position in relation to the major circulation features of the southern hemisphere. The subcontinent lies within the subtropics and its climate is influenced by systems of both tropical and extra-tropical origin (Tyson, 1986; Levey, 1993). Surface-air temperature fields change in response to climatic controls, and the variation from the mean pattern throughout the year is a function of the prevailing airflow type (Taljaard, 1996). With subtropical anticyclonic airflow, positive temperature anomaly fields are predominant, except in local coastal regions where airflow is onshore. With westerly cyclonic disturbances temperature anomaly fields reverse, and negative temperature departures predominate. In all seasons and with all airflow types the temperature anomaly gradient is directed along mean streamlines of airflow (Lengoasa, 1988) and positive anomalies occur in the direction of the wind with increasing distance from the coastline over which the air first crosses the subcontinent. It is quite clear that air circulation over South Africa is among the major determinants of spatial patterns of surface temperature fields.

Horizontal distribution of temperature over the earth's surface is a function of both location properties and the energy transferred by the oceans and atmosphere. South Africa is situated south of latitude 22°30'S and is bounded by oceans on all sides except the north. Because of the different ocean characteristics, air masses with significantly different properties predominate around the west, south and east coasts of southern Africa. Subsequently the frequent influxes of these air masses on to the plateau are likely to create temperature and humidity gradients over land. From the south-western Indian Ocean, with the accompanying warm Agulhas current warm, moist air is fed into the subcontinent from the east and south-east. Cold upwelling on the west coast is responsible for vastly different climatic features. Since the ocean is believed to be the major breeding area for weather and climate of southern Africa, it is understandable that the different characteristics of the oceans surrounding South Africa result in diverse climate features (both rainfall and temperature) over the subcontinent. On the west coast, for example, the annual mean surface-air temperature is about 15°C and on the east coast, on the same latitude, about 21°C. The difference of 6°C is believed to be a direct result of the distinct oceanic features. The annual mean sea-surface temperatures along the east coast is found to be higher than along the west coast. Also, the absolute humidity and average depth of the layer of maritime air on the east coast are both almost double that along the west coast. These factors result in east coast maritime air to be less stable than along the west coast (Taljaard, 1996).

Figure 1.2 depicts the annual cycle of monthly mean temperature for St Lucia (east coast), Kimberley (central interior) and Cape Columbine (west coast). From the figure it is clear that the annual curves of mean temperature vary in different regions of South Africa in mainly four respects: *space* (from place to place), *range* (difference between mean summer and mean winter temperatures), *phase* (time of year when highest maximum or minimum temperatures occur) and *symmetry* (or asymmetry, which is defined as the departure from a symmetrical curve) (Schulze, 1965).

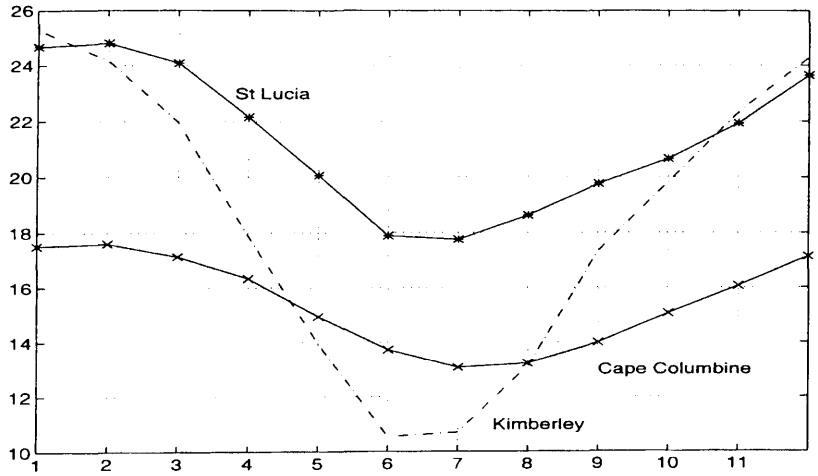

Figure 1.2 Annual cycle of mean temperature for St Lucia (✳), Kimberley (broken line) and Cape Columbine (x).

Space

In January the lowest temperatures follow the Drakensberg range from the Northern Province (Figure 1.3), across the Lesotho massif to the Eastern Cape, and then westwards from the Stormberg to the Roggeveld ranges (Western Cape). The warmest regions are the Orange River Valley, Limpopo Valley, Tugela River Valley and the Lowveld (eastern Mpumalanga and eastern Northern Province). During summer months, the Great Karoo (southern parts of Northern Cape and parts of Western and Eastern Cape) and Little Karoo (Western Cape) are also classed as hot, but the annual variation of temperatures in these areas result in them being colder than the south coast in winter (Schulze, 1965). Low temperature along the west coast occur in contrast with the high temperature of the adjacent interior, resulting in a steep temperature gradient between coast and interior. The mean temperatures along the south and east coasts differ very little from those of the adjacent interior. A belt of relative high temperature is found immediately seawards from the main escarpment of the Eastern Cape.

The regional distribution of the duration of summer shows that the summer season is shortest on the south coast and increases in length towards the north. The outstanding feature, however, is that summer lasts longer over the eastern Highveld than over the western interior in the same latitude. One reason being the annual march of sunshine duration, which is also closely related to solar radiation and cloudiness (Taljaard, 1996).

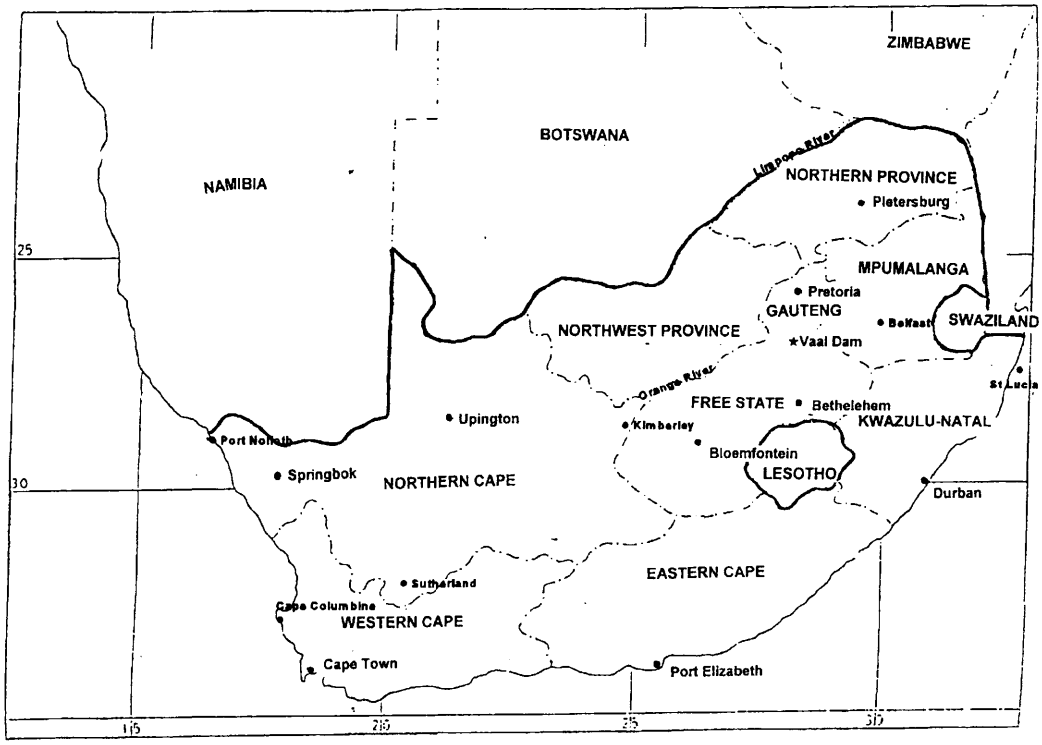

Figure 1.3 Provincial map of South Africa.

The coldest areas in South Africa (during all months) are confined to the edge of the great escarpment, from Sutherland (southern parts of Northern Cape) to north of Belfast (Mpumalanga), as well as right on the west coast. The major contrast between land and sea which exists along the west coast in summer, disappears in winter. The east and south coasts are warm zones in winter.

Range

The highest annual variation of mean maximum and minimum temperatures is found in the western interior and decreases to the coast and to the north. The smallest variation in mean temperature is found on the north-west coast near Port Nolloth. At coastal stations, the minimum temperatures are inclined to be stable and not subject to large fluctuations, while the maximum temperature tends to show occasionally large extremes. In the interior the opposite is shown to be the case (Schulze, 1965). This is in accord with the fact that the coastal belt is subject to occasional hot berg winds, whereas the interior suffers from periodic influences of cold subantarctic air.

The effect of cloudiness is to reduce the amount of solar radiation reaching the surface during daytime. Generally, if a cloud layer persists for a long period, the surface temperature remains well below its normal daily cycle. On the other hand, cloud cover at night tends to raise the minimum temperature by several degrees because of the absorption effects at the surface and the insulating effects of the clouds. The result is that under cloudy conditions the difference between maximum and minimum temperature is greatly reduced. The effect of increased cloudiness upon mean temperatures against the eastern escarpment is reflected in the decreased range of temperatures in that area (Schulze, 1965).

Phase

Air temperature is very much affected by the absorption of solar energy by the atmosphere and the long wave earth radiation. There is not, however, a one-to-one relationship in time between highest solar input and highest temperatures on a daily or seasonal scale (Tyson, 1986). Earth revolution causes maximum and minimum insolation to occur at the time of solar solstices in each hemisphere. Thus, June and December represent the time of least and greatest solar receipts respectively in the Southern Hemisphere, but these months are not the coldest or warmest in South Africa. A one to two month lag is common in many parts of the world (Oliver and Hidore, 1984).

In the western parts of South Africa both the maximum and minimum of the annual temperature cycle tend to occur later than in the east. Also, from Figure 1.2, the warmest and coldest months along the west coast (e.g. Cape Columbine) lag those over the interior (e.g. Kimberley) by about a month. Similar features hold true for other stations as well. The different thermal properties of water and land cause a large phase shift in mean temperatures along coastal regions.

Symmetry

Asymmetry (the departure of a station's temperature curve from a symmetrical curve) increases northwards over the country. Over the Highveld the asymmetry is greater than over the western interior. This is mainly because spring temperatures in the northern regions are higher than those indicated by a symmetrical curve. In the Great Karoo an almost perfect sine curve in the mean temperature variation is evident. This is a result of the cloudless conditions which exist

almost throughout the year over the western interior. On the coasts the annual variation of mean temperature is delayed due to the influence of the oceans which only respond with a period of a month or more to external heat output.

Anomalously hot or cold periods are common features in South Africa, but are generally of short duration (two to three days). Warm episodes tend to last somewhat longer than colder periods. The most intense warm periods also last longer than those of lesser intensity, which is contrary to the behaviour of cold spells. Long lasting warm spells are generally a result of a persistent synoptic circulation such as a strong upper-air high pressure system accompanied with subsidence over the continent. A tropical cyclone lingering in the Mozambique channel may also cause subsidence over the eastern and north-eastern regions that could last a number of days. Cold spells are usually the result of an extra-tropical cyclone and accompanying cold front activity that moves across the country. Cold or warm spells do not show a particularly well marked seasonal change in frequency, but the tendency during summer is for the greatest number of cold spells to occur over the south-eastern and eastern escarpment, whereas in winter a predominance of cold spells is indicated over the western parts. Cold air invasions in winter therefor seem to enter South Africa more directly from the west, while in summer cold air reach the interior over the escarpment from the southeast and east. This is mainly due to the seasonal shift of the subtropical high pressure belt (Schulze, 1965).

On a climatological timescale, the tendencies of the southern hemisphere temperature records reveal an increase in temperatures with a warming of about 0.6°C between 1880 and 1980 (Hansen and Lebedeff, 1987). The highest rate of warming in the southern hemisphere occurred since 1965. Monthly mean temperatures over the period 1940-1989 show little evidence of any trend over South Africa and only a few coastal regions had significant temperature increases. Studies on seasonal and monthly time scales revealed that minimum temperatures, however, have been increasing in the north in spring, whereas for stations further east no specific trend is apparent over the period 1940-89 (Mühlenbruch-Tegen, 1992). Also, in summer positive trends have been confined to the north-west. When comparing temperature trends over South Africa with those of rainfall, a negative correlation is found at all stations (Schulze, 1965).

1.3 Relation Between Sea-surface Temperature and Surface-air Temperature

It is accepted that oceans play a vital role in global climate (Barnett *et al.* 1994; Barnston. 1994; and others). This is because the oceans have a large thermal inertia and act as a heat and moisture source for the atmosphere. In its own right, the El Niño/Southern Oscillation (ENSO) phenomenon is intensively researched because of its large effects on the climate and economy in various regions of the world. The southern oscillation (SO) refers to an atmospheric pressure fluctuation which oscillates at two centres that are thousands of kilometres apart. This oscillation in the surface pressure field across the Pacific ocean is associated with major changes in rainfall and temperature patterns and wind fields in all parts of the world (Philander, 1990; Barnett *et al.*, 1991; Glantz *et al.*, 1991). The term 'EL Niño' has become reserved for the sequence of changes in the circulation across the Pacific ocean and Indonesian archipelago when sea-surface warming is particularly strong. The analysis of ENSO response in surface-air temperature (and precipitation) is difficult because the magnitude and extent of surface ENSO-related signals may vary from episode to episode.

Much of the work relating the SO to surface parameters has focussed on precipitation. Regarding temperature, Walker and Bliss (1932) indicated southern oscillation-temperature relations in some regions of the globe. SO-temperature correlations indicate that the strongest relationships between SO and temperature occur in the tropics. Berlage(1966) found some relationships between the high-phase SO 'relaxations' and northwest European cold winters. Newell and Weare (1976) first showed that tropical temperature anomalies in the troposphere are in phase with sea-surface temperature (SST) anomalies in the equatorial Pacific. Outside the tropics, relationships between the phase of ENSO and temperatures are not as well defined as the tropical responses and are rather an indirect result through tropical forcing of circulation patterns. Work relating ENSO and surface-air temperature variations has been performed by van Loon and Madden (1981), Kiladis and van Loon (1988) and Kiladis and Diaz (1989). Recently, Halpert and Ropelewski (1992) presented a comprehensive examination of the temperature patterns associated with the high and low extremes of the SO. They concluded that ENSO does influence surface temperatures on regional to global spatial scales, with greatest effect in the tropics.

In the tropics surface-air temperature anomalies are in general of the same sign as the underlying equatorial sea surface temperature (SST) anomalies. During warm episodes (El

Niño), surface-air temperatures are above-normal in the eastern equatorial Pacific. Conversely, ambient temperatures in this region are below-normal during cold events (La Niña). In the south-central and western Pacific Ocean, air temperatures are anomalously cold during warm episodes and warm during cold episodes, as this region experience SST anomalies out of phase with those in the central and eastern Pacific (Rasmusson and Carpenter, 1982). The general increase or decrease in surface temperature throughout the global tropics is a delayed response to the warming or cooling of the equatorial SSTs, primarily in the Pacific. In some continental subtropical regions, such as southeast Africa, the sea-surface and ambient temperature relationships are probably influenced by variations in cloud cover, adiabatic warming in the subsiding air and advection (Lengoasa, 1988). These areas were found to generally experience above-normal seasonal temperature during anomalously warm conditions in the equatorial Pacific Ocean when it is also anomalously dry over the subcontinent, and below-normal seasonal temperature (above-normal precipitation) during anomalously cold conditions (Ropelewski and Halpert, 1987; 1989).

1.4 Seasonal Temperature Forecasting

Status

The status and use of long-range predictions (e.g. monthly and seasonal averages of temperature and precipitation) have often been the subject of debate in meteorological literature (e.g. Barnston and Livezey, 1989; Chervin and Bettge, 1983; 1985; Barnett *et al.*, 1994). Such reliable and accurate forecasts would be enormously valuable in any number of venues (Knox *et al.,* 1985). However, indications are that long-range skill is likely to be highly localised, with particular regions, seasons, regimes and phenomena contributing to predictable signals in a generally noisy record. This opinion has been shared by both producers (Gilman, 1985) and users (Knox *et al., 19*85) of long-range forecasts alike, and also the broader meteorological community. In fact, the policy statement of the American Meteorological Society (AMS) (1983) asserts that " *at longer ranges....typically a month or season.... forecast skill is small*" and that "*slight skill exists in forecasting average temperature for the month or season".* However, the AMS goes on to say that "*even small improvements should be of substantial economic benefit*". The idea is supported by studies such as Katz *et al.* (1985) arguing that the relationship between quality (skill and accuracy) and the value of long-range predictions is highly non-linear. Any small gain in quality might enhance the value of long-range predictions considerably.

Predictions of the seasonal behaviour of the atmosphere are made using empirically- and physically-based models. Physical models attempt to forecast the time-averaged future atmospheric conditions by simulating the dynamic and thermodynamic processes which determine the state of the overlying atmosphere. Empirical models rely on past statistical associations between lower-boundary forcing or atmospheric precursors and the climatic variable being forecasted (Barnett and Preisendorfer, 1987; Hastenrath, 1990a; b; Chu and He, 1994).

Coupling between ocean and atmosphere in the tropical regions are more direct than in the extra tropics (Gill, 1980; Livezey, 1990a; b). Local efforts, utilizing general circulation models (GCM), have been restricted in determining the response of the atmospheric circulation to SST boundary forcing (Jury *et al.*, 1996; Rautenbach, 1997; van Heerden and Rautenbach, 1997). Therefore, extra tropical seasonal predictions remain largely an empirical exercise. Speculation has recently focused on the possibility that coupled GCMs could extend the range of dynamic predictability, but practical application of such models to extra tropical prediction is still in its infancy (Livezey, 1990a; Tennant, 1997). To predict the behaviour of seasonal climate, statistical methods are mainly used in which regression equations relate the atmospheric conditions to a set of historical data. By analogy with the relative mature subject of shorter range predictability, it may be anticipated that the understanding of long-range predictability will be advanced by a combination of theoretical, empirical and numerical methods. Thus, with increasing physical understanding, dynamically based forecasts have the potential to become more skilful than purely statistical ones. Currently however, the two approaches deliver roughly equally skilful forecasts, and the simplest, less costly model performs about as well as the more comprehensive models (Barnston, 1994).

The possibilities for forecasting seasonal surface-air temperature for different regions of the world have been examined in several studies. Harnack (1979) used multiple linear regression to forecast USA winter temperature from prior SST and atmospheric circulation anomalies. Harnack (1982) demonstrated that the level of forecast skill for temperatures showed regional variations. Barnett (1981) also examined the predictability of USA seasonal air temperatures using multiple regression with Pacific SST and sea-level pressure (SLP) as predictors. Skill of the forecasts was generally low and varied with season and location. ENSO-related winter-temperature predictions for the USA have been developed during the past decade on the basis of an improved understanding of variations in the strength, timing and type of ENSO events (Barnett and Preisendorfer, 1987; Barnett *et al.*, 1994; Halpert and Ropelewski, 1992; Barnston and Smith, 1996).

Users

The potential pay-off of even moderate increases in accuracy of monthly to seasonal temperature predictions is realized by the energy industry (Knox *et al.,* 1985), agribusiness (Sonka *et al.,* 1988) and by decision makers in the economic community. As Knox *et al.* (1985) pointed out, peak demands for gas space heating in the USA are sensitively dependent on temperature and its extremes. The same applies for the electricity industry in South Africa. Low ambient temperature implies heavy use of electricity with sizable amounts drawn, especially in high populated areas. On the other hand, an unusually warm winter may lead to a glut and high storage costs due to carryover. During an extremely hot summer, a high demand for electricity is evident once again. This time mainly for the use of air-conditioners to maintain a acceptable indoor climate. The storage of power (electricity, coal, gas, oil) is a costly business and the extent to which such stock should be build up is determined by the estimated maximum demand, which is closely related to surface-air temperature. The electricity manager is specifically concerned about extremes of temperature in both long-term and short-term planning. The most relevant forecasts are for above- and below-normal temperature in summer- or wintertime in a particular region (Knox *et al.*, 1985).

Survey operations, either on land or from the air, are subject to weather conditions. Initial planning can help to select the correct time of year and to estimate the time needed to complete the survey. Work in certain hot, humid climates can be a potential health risk (causing for example heat exhaustion or dehydration). In this regard the continuation of construction work, or other outdoor activities, may be hampered. The same applies for extremely cold conditions. The dangers involved in mining can be greatly increased under certain temperature (and rainfall) conditions. Coal, for example, cannot be delivered easily under extreme cold conditions.

Some industries are dependent on the weather and climate for the volume of their sales, thus their whole production must be geared to current and future conditions. This is true for the ice-cream and soft drink industries. More cold drinks and ice-cream are sold during extremely hot periods. If a knowledge of expected monthly or seasonal conditions can help in the planning process so that the availability could reach the demand, these industries will benefit from such forecasts.

Many other industries such as manufacturers of clothing and perishable foods with a profound seasonal demand could benefit from skilful seasonal temperature predictions. With international

trade becoming more and more important, knowledge of the influence of climate becomes essential not only in the design and specification of the articles, but also in their packaging and transport over long distances.

Adverse temperatures result in direct stress to animals. In the dairy farming industry milk production is related to temperature (WMO, 1994) and cold stress might even cause mortality. Also, poultry growth is related to temperature, among other climatic elements. Crop farmers in areas of winter rainfall in South Africa where the cold season is the main growing season, are especially interested in winter temperature predictions. Insect population displays a high degree of sensitivity to ambient temperature and they generally increase during warm and humid periods, causing a higher pest population. Various operations such as planting, irrigation, harvesting, burning, disease control etc. could be planned with an adequate knowledge of expected seasonal conditions in hand.

These are but a few potential users who may benefit from seasonal temperature predictions. More applications of seasonal temperature forecasts may exist, but the extent of these in South Africa will only become known once reliable forecasts become available.

In summary, forecasts of mean temperature conditions for up to a season is possible with considerable reliability for certain parameters, places, seasons and situations, thereby making them potentially beneficial for certain users. These views, and the fact that prospects do exist for improvements in long-range forecast skills, provide considerable justification for the continued support of research and development of climatic fluctuation predictions. Additionally, research documents of real forecasts (e.g. Preisendorfer and Mobley, 1984; Barnet and Preisendorfer, 1987) leave little doubt that such forecasts are possible. Thus, one can conclude that skilful long-lead forecasts can be made, but with modest accuracy. Furthermore, small gains in this accuracy are possible with potentially large increases in economic value for certain applications.

1.6 Aims of the Research

It may be possible to match seasonal forecasts to applications with substantial economic pay-off. To date seasonal forecasting efforts in South Africa have concentrated on rainfall and attempts to provide seasonal forecasts for temperature are in the early stages of development (Mason *et al.*,1996). This study aims at setting a framework against which further research and improvements could be made.

The aims of this research are:

1) To show that global scale sea-surface temperatures are predictors of South African seasonal temperature.
2) To identify the important ocean regions that contribute to forecast skill.
3) To investigate the effect of important sea-surface temperature modes on South Africa's seasonal temperature.
4) To construct a statistical forecasting model for seasonal temperature over South Africa.
5) To verify that this model is able to predict seasonal temperature with significant skill.

The main aim is then to set up a scheme to forecast seasonal air-temperature over South Africa. The methods and data used in this study are discussed in Chapter 2. In Chapter 3 singular value decomposition is used to identify significant centres in the ocean that are related to South African seasonal surface-air temperatures. The atmospheric response to certain ocean temperature forcing will be discussed in Chapter 4, with specific reference to circulation patterns over South Africa. A model to predict seasonal surface-air temperature at 77 different locations in South Africa is developed in Chapter 5 with the implementation of a statistical technique namely canonical correlation analysis. This statistically based forecast model is tested and evaluated in Chapter 6 to determine if these predictions are skilful and thus useful in the South African scenario. All the findings and some recommendations are summarized in Chapter 7.

CHAPTER 2

DATA AND METHODS

2.1 Introduction

Sea-surface temperatures variability are held responsible for a large percentage of mean temperature variability world wide (Barnett, 1981; Barnett and Preisendorfer, 1987; Halpert and Ropelewski, 1992; Barnston and Smith, 1996). Monthly sea-surface temperature data will be used in this study as a predictor in a statistically based model to predict seasonal surface-air temperatures in South Africa. A description of the data and other multivariate techniques that will be used in the analysis, follows below.

2.2 Data

In this study the potential to forecast seasonal surface-air temperatures for South Africa by using sea-surface temperatures from different ocean areas is investigated. Two sets of data are therefore needed to construct such a model, namely surface-air temperature over South Africa (predictand data) and sea-surface temperature (predictor data). The atmospheric response to certain sea-surface temperature conditions is investigated and the dataset used to analyse the atmospheric patterns is described.

Surface-air Temperature Data

Mean monthly maximum temperature data at 77 temperature observation stations over South Africa are used. The temperature data set is obtained from the South African Weather Bureau. All these stations have a complete and quality-controlled maximum temperature record for the period 1960 to 1995. The spatial distribution of the temperature stations is shown in Figure 2.1.

Over the 36-year period, correlation between maximum and minimum monthly mean temperatures were found to be above 0.84 at all stations with corresponding records. Figure 2.2 shows that in more than 75% of the cases, correlations of above 0.9 exist between monthly

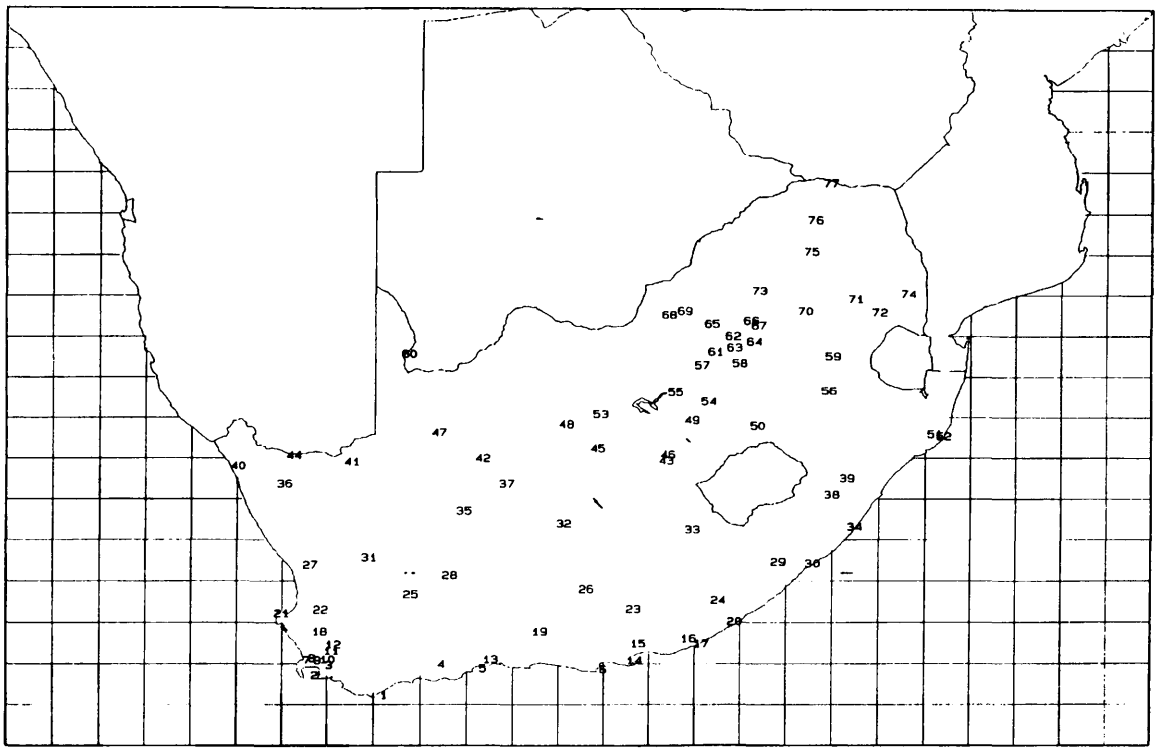

1	CAPE AGULHAS	27	VREDENDAL	53	VAALHARTS
2	CAPE POINT	28	FRASERBURG	54	KROONSTAD
3	SOMERSET WEST	29	UMTATA	55	BOTHAVILLE
4	RIVERSDALE	30	CAPE HERMES	56	VOLKSRUST
5	CAPE ST BLAIZE	31	CALVINIA	57	POTCHEFSTROOM
6	CAPE ST FRANCIS	32	DE AAR	58	VEREENIGING
7	KIRSTENBOSCH	33	ALIWAL NORTH	59	NOOITGEDACHT
8	CAPE TOWN-ASTRON	34	PORT SHEPSTONE	60	GEMSBOKPARK
9	CAPE TOWN D.F.MALAN	35	VAN WYKSVLEI	61	CARLETONVILLE
10	JONKERSHOEK	36	SPRINGBOK	62	KRUGERSDORP
11	PAARL	37	PRIESKA	63	ZUURBEKOM
12	WELLINGTON	38	EMERALD DALE	64	JAN SMUTS
13	GEORGE	39	CEDARA	65	RUSTENBURG
14	PORT ELIZABETH	40	PORT NOLLOTH	66	PRETORIA
15	ADDO	41	POFADDER	67	PRETORIA - UNIV
16	BATHURST	42	BOEGOEBERGDAM	68	MARICO
17	GREAT FISH POINT	43	BLOEMFONTEIN	69	LINDLEYSPOORT
18	LANGGEWENS	44	HENKRIESFONTEIN	70	LOSKOP DAM
19	WILLOWMORE	45	KIMBERLEY	71	LYDENBURG
20	EAST LONDON	46	GLEN COLLEGE	72	NELSPRUIT
21	CAPE COLUMBINE	47	UPINGTON	73	WARMBATHS
22	HELDERVUE	48	KOOPMANSFONTEIN II	74	SKUKUZA
23	SOMERSET EAST	49	VIRGINIA	75	PIETERSBURG
24	DOHNE	50	BETHLEHEM	76	MARA
25	SUTHERLAND	51	RIVER VIEW	77	MESINA
26	GRAAFF-REINET	52	CAPE ST LUCIA		

Figure 2.1. Distribution of maximum temperature stations in South Africa.

mean maximum and minimum temperatures. A complete record of maximum temperatures since 1960 exists for 77 stations as opposed to 61 stations with complete minimum temperature records for this period. It was therefore decided to use the larger set of 77 stations in this study.

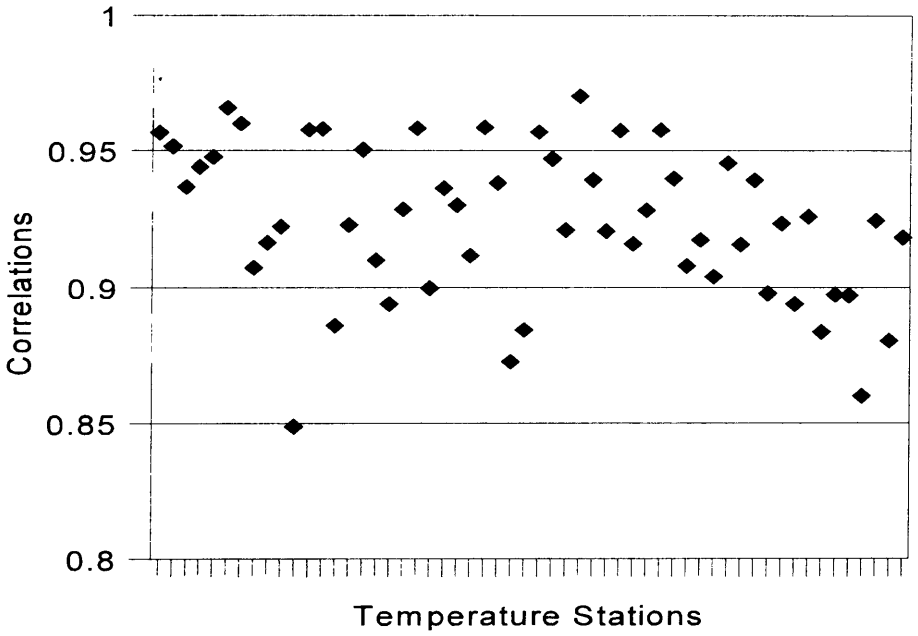

Figure 2.2. Correlation between minimum and maximum monthly mean temperature at 56 temperature stations with complete records for the period 1960 to 1995.

Sea-surface Temperature Data

Three sea-surface temperature (SST) data sets for the period 1960 to present are used. For the period January 1946 to February 1986 the Global Ocean Global Atmosphere (GOGA) monthly mean sea-surface (SST) analysis is used (Pan and Oort, 1990; Lau and Nath, 1994). This is a global data set with resolution 7.5° x 4.5°.

The Blended SST Analysis data set, on a 2-degree latitude and longitude grid, from the Climate Prediction Center is used for the period 1982 to 1994. The fields are compiled from a blend of *in situ* data, satellite and ice data. A complete description of the data analysis procedures is given by Reynolds (1988) and Reynolds and Marsico (1993).

The optimum interpolation (OI) SST data set is used from January 1995, and is available on a 1-degree grid. This analysis uses *in situ,* ice data and satellite derived SST data. A description of the OI analysis can be found in Reynolds and Smith (1994). The OI data is also used to make operational seasonal temperature forecasts for South Africa.

For the purpose of this study the SST data from the three fields described above were combined as follows: for the period 1959 to 1984 the GOGA data is used, from 1985 to 1994 the Blended data is implemented, and from 1995 to present the OI data is used. All the data are interpolated to a 7.5 x 4.5 degree grid using cubic interpolation. A total of 440 gridpoints are used from the ocean areas known to influence South Africa's climate (Jury *et al.*,1996; Mason, 1992; Landman, 1997; Rautenbach, 1997) namely the equatorial Pacific Ocean (20°N to 20°S), the Indian Ocean (to 45°S) and the southern Atlantic (5°N to 45°S).

Atmospheric Data

Sea-level pressure and 500 hPa geopotential data are used to analyse the atmospheric circulation patterns during certain years. The dataset used is the National Centers for Environmental Prediction (NCEP) reanalysis data. The data is on a 2.5 x 2.5 degree grid. Monthly mean data are extracted between 20° to 35°S and 10° to 35°E for a grid over South Africa.

2.3 Methods

Principal Component Analysis

Principal component analysis (PCA) is a widely used technique in meteorology (Richman, 1986; Sneyers and Goossens,1987; Jolliffe, 1990, Jackson, 1991; Peixoto and Oort, 1992). In the South African context PCA was used to research rainfall variability (Mason,1992; Landman, 1997; Landman and Mason, 1997). In this study PCA will be used to investigate the seasonal variability of surface-air temperature in South Africa, and to pre-filter the model input data.

The method of principal components is primarily an eigenvalue/eigenvector technique which obtains linear transformations of a group of correlated variables in order to achieve certain optimal conditions. A typical data set can be viewed as *n* observations measured on *p* variables. Often the *p* variables are highly correlated, which implies that most of the variance could be

represented by less than p variables. PCA is a method used to reduce these p variables to an optimal number m (where $m \leq p - 1$) by means of a linear function.

A linear function of the p variables will be of the form $z = \alpha_1 x_1 + \alpha_2 x_2 + \ldots + \alpha_p x_p$ where α_1, α_2, ..., α_p are coefficients and x_1, x_2, ... ,x_p are the p variables. Different sets of coefficients (or eigenvectors) will result in different linear functions of which the variance can be calculated. The first principal component is that linear function which has the maximum possible variance, the second principal component is the linear function with maximum possible variance subject to orthogonality with the first principal component, and so on.

Selection Rules

The next step will be to determine m - the optimal number of principal components (PCs) that describes the original data set adequately. A large number of criteria are in use (Jackson, 1991). In this study the Guttman-Kaiser criterion, also known as the Average Root, is used. This technique retains only those principal components that account for more variation than the avarage variation in the original variables. In this study correlation matrices are used, in which case the average root will be 1.

Another, often used objective selection rule to determine the number of physical significant PCs is applied, namely Rule N (Preisendorfer *et al.*, 1981; Preisendorfer, 1988). For Rule N, eigenvalues which are significantly larger than that of a cumulative distribution of a number of centred random data sets, are considered significantly better than noise-eigenvalues. Rule N is known to under selects the number of PCs, while the Guttman-Kaiser technique tends to retain more PCs that are manageable in large datasets (Jollife, 1993).

Singular Value Decomposition

Singular value decomposition (SVD) is one of several methods (Bretherton *et al.,* 1992) for the simultaneous statistical analysis of two quantities which vary in both space and time. Although not widely used in meteorology, SVD is a simple method to perform, results are easily interpreted and are similar to more elaborate methods such as combined PCA (Bretherton *et al.*, 1992). SVD was first used in a meteorological context by Prohaska (1976) to document the simultaneous relationships between monthly mean surface air temperature over the United States and hemispheric sea-level pressure patterns. It was subsequently used by Lanzante

(1984) and Dymnikov and Filin (1985) to document certain meteorological relationships. In this study SVD is used to investigate the effect of the sea-surface temperatures of different oceans on South African mean seasonal maximum surface-air temperature (T_x).

SVD is a method to isolate important coupled modes of variability between time series of two fields called a *left data field* and a *right data field*. Consider a *left data field* **s**(x,t) that consists of τ observations, each of which has N_s grid points, and a *right data field* **z**(y,t) with the same number of observations (τ) at N_z grid points (or stations). The fields can be viewed as N_s X τ and N_z X τ matrixes respectively (Figure 2.3).

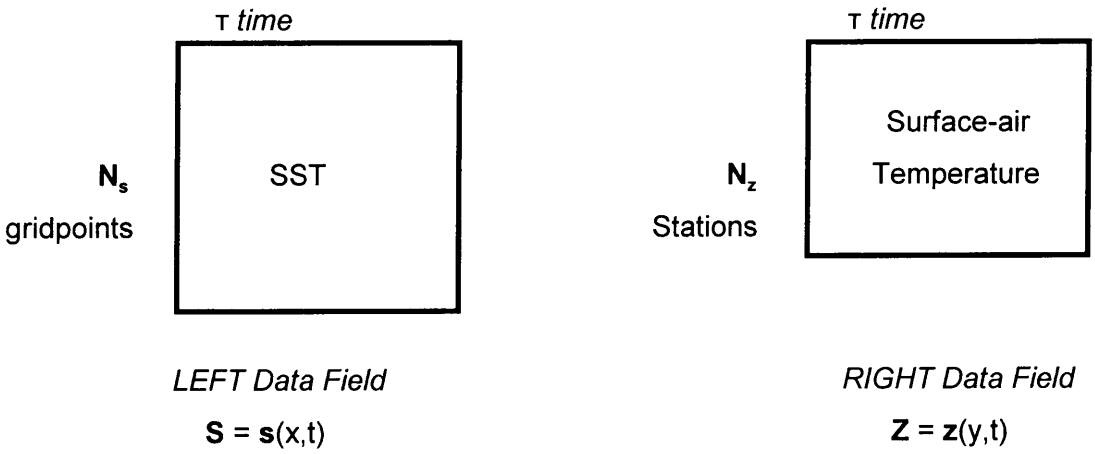

Figure 2.3. Schematic presentation of left and right data fields.

Any analysis of the coupling between the left and the right data fields will only provide meaningful results if there are significant correlations between some elements of **S=s**(x,t) and **Z=z**(y,t). The data time series **s**(x,t) and **z**(y,t) at each of the gridpoints can be expanded to determine a set of vectors, called *patterns* ($\boldsymbol{p}_k$ and $\boldsymbol{q}_k$) so that the covariance between projections of **s**(x,t) on $\boldsymbol{p}_k$ and projections of **z**(y,t) on $\boldsymbol{q}_k$ are maximized. The covariance between **s**(x,t) and **z**(y,t) can be decsribed by the equation:

$$\boldsymbol{p}_k^T \boldsymbol{C}_{sz} \boldsymbol{q}_k = \sigma_k \qquad (2.1)$$

where $\boldsymbol{p}_k^T$ is the transposed of $\boldsymbol{p}_k$ and

$$\boldsymbol{C}_{sz} = \frac{1}{T}\boldsymbol{S}\boldsymbol{Z}^{T} \tag{2.2}$$

is a N_s X N_z temporal covariance matrix and σ_k is a Lagrange multiplier that measures covariance between the two fields for the *k*th mode (Cheng and Dunkerton, 1995).

Having defined the singular vectors $\mathbf{p}_k$ and $\mathbf{q}_k$, the data fields can be decomposed as follows:

$$\boldsymbol{s}(x,t) \equiv \sum_{k=1}^{N} a_k(t)\boldsymbol{p}_k(x) \tag{2.3}$$

$$\boldsymbol{z}(y,t) \equiv \sum_{k=1}^{N} b_k(t)\boldsymbol{q}_k(y) \tag{2.4}$$

Where the *expansion coefficients*, a_k and b_k, are calculated as weighted linear combinations of the grid point data:

$$a_k(t) = \sum_{i=1}^{N_s} u_{ik}s_i(x,t) = \boldsymbol{u}_k^{T}\boldsymbol{S} \tag{2.5}$$

$$b_k(t) = \sum_{j=1}^{N_z} v_{jk}z_j(y,t) = \boldsymbol{v}_k^{T}\boldsymbol{Z} \tag{2.6}$$

The vectors $\mathbf{u}_k$ and $\mathbf{v}_k$ are called *weight vectors*. These vectors are constrained to be mutually spatially orthogonal, so that the patterns are the same as the weight vectors. In other words, for SVD $\mathbf{u}_k = \mathbf{p}_k$ and $\mathbf{v}_k = \mathbf{q}_k$.

Each pair of patterns (or weight vectors) and the corresponding pair of expansion coefficients define a *mode*. The relative importance of a SVD mode can be measured in terms of the squared covariance fraction (SCF). The total squared covariance of a single pair of patterns isso that the SCF, or the fraction of the squared covariance explained by a certain pair of patterns, is defined as:

$$SCF = \frac{\sigma_k^2}{\sum_{l=1}^{r} \sigma_l^2} \tag{2.7}$$

The leading patterns $\mathbf{p}_1$ and $\mathbf{q}_1$ are chosen so that the projection $a_1(t)$ of $\mathbf{s}(x,t)$ on $\mathbf{p}_1$ has the maximum squared covariance with the projection $b_1(t)$ of $\mathbf{z}(y,t)$ on $\mathbf{q}_1$. Successive pairs ($\mathbf{p}_k$, $\mathbf{q}_k$) are chosen in the same way with the added condition that $\mathbf{p}_k$ is orthogonal to $\mathbf{p}_1$, ... , $\mathbf{p}_{k-1}$ and $\mathbf{q}_k$ is orthogonal to $\mathbf{q}_1$, ... , $\mathbf{q}_{k-1}$. The *first* mode indicates the maximum explained variance, the *second* mode, the second highest explained variance, and so forth.

Using the expansion coefficients a_k and b_k two types of correlation maps can be generated, namely *homogeneous maps* and *heterogeneous maps*. The *k*th *left* homogeneous correlation map is defined to be the vector of correlations between the grid-point values of the *left* data field and the *k*th *left* expansion coefficient. This map is a useful indicator of the geographic location of the covarying part of the *left* field.

Similarly, the *k*th *left* heterogeneous correlation map is the vector of correlations between the grid-point values of the *left* data field and the *k*th expansion coefficient of the *right* field. This map indicates how well the gridpoints in the *left* field can be predicted from the *k*th *right* expansion coefficient. The same applies for the *right* homogeneous and heterogeneous maps.

Canonical Correlation Analysis

Canonical correlation analysis (CCA) is a method originally developed by Hotelling (1936). It is known to be at the top of the hierarchy of regression modelling approaches (Barnett and Preisendorfer, 1987). The first meteorological application of CCA was by Glahn (1968), who used it in the context of statistical weather prediction. It was recently used in meteorology by

Barnett and Preisendorfer (1987), Nicholls (1987), Barnston (1992, 1994), Chu and He (1994), Renwick and Wallace (1995). In the South African context CCA was used to construct forecast models for seasonal rainfall (Barnston and Smith, 1996; Landman, 1997; Thiao and Barnston, 1997). In this study the CCA technique is used as a forecasting tool to predict seasonal mean maximum surface-air temperature in South Africa from a sea-surface temperature predictor field.

CCA is a technique that isolates the linear combination of data from the *left data field* (as in Figure 2.3) and the linear combination of the *right data field* that have the maximum correlation. This pair of time series may be more strongly correlated than the expansion coefficients of the leading pair of patterns deduced from SVD, but explains a smaller fraction of the covariance between the two fields.

In CCA the expansion coefficients are constrained to be temporally uncorrelated, but in general the weight vectors are not spatially orthogonal. Hence, the patterns are not the same as the weight vectors as is the case with SVD. Here the weight vectors (Equations 2.5 and 2.6) indicate which grid-point values are dominant in forming the expansion coefficient. As is the case with SVD the weight vectors and correlation maps are important pairs of fields to examine when using CCA.

In this study the time series of each data field is filtered by projection onto a leading subset of its principal components and then the maximum correlation between linear combinations of the filtered time series of the two fields is sought. The theory is extensively decribed by Tatsuoka (1988), Jackson (1991) and Chu and He (1994). Consider a predictor dataset **X** (ex. 3-month mean global scale sea-surface temperatures) and a predictand data set **Y** (ex. seasonal mean surface-air temperature at different locations). The dimension of **X** (*p*) and **Y** (*q*) are such that $q \leq p$. These datasets can be decomposed into their principal components and then the set of canonical vectors (**u**,**v**) are obtained. By solving the eigenvalue problems:

$$(\boldsymbol{S}_{xx}^{-1}\,\boldsymbol{S}_{xy}\,\boldsymbol{S}_{yy}^{-1}\,\boldsymbol{S}_{yx} - \lambda^2\boldsymbol{I})\boldsymbol{u} = 0 \qquad (2.8)$$

and

$$(\boldsymbol{S}_{yy}^{-1}\,\boldsymbol{S}_{yx}\,\boldsymbol{S}_{xx}^{-1}\,\boldsymbol{S}_{xy} - \lambda^2\boldsymbol{I})\boldsymbol{v} = 0 \qquad (2.9)$$

where $\mathbf{S}_{xx}$ (pxp) and $\mathbf{S}_{yy}$ (qxq) are the sums of squares and cross-products from the predictor (**X**) and predictand (**Y**) matrices (non-singular); $\mathbf{S}_{xy}$ (pxq) and $\mathbf{S}_{yx}$ (qxp) are the sum of products between the two matrices and ***I*** is the identity matrix; the eigenvalue (λ_i) and the corresponding predictor eigenvector ($\mathbf{u}_i$) could be linearly combined. The eigenvector/eigenvalue pair with the highest correlation forms the fist canonical mode, the following canonical modes will be less strongly correlated and orthogonal to the previous found pairs.

Subsequently the prediction equations can be solved (Glahn, 1968):

$$\hat{\boldsymbol{Y}} - \bar{\boldsymbol{Y}} = [(\boldsymbol{V}')^{-1} \Lambda \boldsymbol{U}'] (\boldsymbol{X}-\bar{\boldsymbol{X}}) \qquad (2.10)$$

where $\hat{\boldsymbol{Y}}$ is the predicted value, $\bar{\boldsymbol{Y}}$ and $\bar{\boldsymbol{X}}$ are temporal mean values and $\boldsymbol{X} - \bar{\boldsymbol{X}}$ the predictor anomaly. $\boldsymbol{U}' = (u_1', u_2', \ldots, u_q')'$ and $\boldsymbol{V}' = (v_1', v_2', \ldots, v_q')'$ where u_1 and v_1 are the first canonical vectors, u_2 and v_2 are the second canonical vectors, etc. and Λ is the diagonal matrix of eigenvalues with $\lambda_1 \geq \lambda_2 \geq \ldots \geq \lambda_q$.

Determination of Forecast Skill

The procedure to test the skill of models used in this study is known as *cross-validation* (Michaelsen, 1987; Barnett and Preisendorfer, 1987; Barnston and Livezey, 1989; Barnston and Ropelewski, 1992). In this procedure forecast models are developed using only part of the available data to predict for the remaining years. Table 2.1 shows the principles of cross validation used in this study:

Table 2.1 Cross validation scheme.

	Year 1	Year 2	Year 3	...	...	Year *n-1*	Year *n*
Case 1							
Case 2							
Case 3							
...							
Case *n*							

For *Case 1* withdraw from the predictor (SST) and predictand (T_x) datasets the values for *Year 1*. Use the remaining *n-1* predictor datapoints to construct a model and predict T_x for *Year 1*. For *Case 2*, withdraw the data for *Year 2,* using *Year 1* and *Year 3* to *Year n* to construct a new model to predict T_x for *Year 2.* Continue to case *n* to obtain *n* independent predictions from the model.

The predicted and observed data fields are subsequently decomposed into three equally probable sets (or terciles). The percent of categorical correct forecasts at a certain location (i.e. temperature station) is referred to as the *local* skill (S_L) (Barnett and Preisendorfer, 1987) and is defined as:

$$S_L = 100\left(\frac{N_c}{n+1}\right)\ \% \qquad (2.11)$$

where N_c is the number of correct categorical forecasts. By averaging the local scores for each station over the entire country, the average local skill is obtained.

Linear Error in Probability Space Scores

A number of well known evaluation techniques are in use for categorical forecasts such as Heidke scoring (Heidke, 1926), Sutcliffe score (Freeman, 1967), Folland-Painting scores (Folland *et al.*, 1986), ranked probability score (RPS) and hits score (Ward and Folland, 1991; Barnston, 1992). The technique applied to evaluate the independant forecasts is known as linear error in probability space (LEPS). LEPS scoring is regarded as the preferred score for categorical forecasts (Barnston, 1992; Livezey, 1995) and it aims to provide a scoring system that measures the error in a forecast according to the distance between the position of the forecasts and the corresponding observation. Table 2.2 shows the skill coefficients for three equi-probable categories as derived by Potts *et al.* (1996).

Table 2.2. LEPS scores for terciles (after Potts *et al.*).

		Observed Category		
		B	**N**	**A**
Forecast Category	**B**	0.89	-0.11	-0.78
	N	-0.11	0.22	-0.11
	A	-0.78	-0.11	0.89

LEPS scores are used in this study to evaluate forecasts for different seasons. A measure of skill is derived over a range from -100 to 100% with the average skill (SK) defined as follows:

$$SK = 100 \frac{\sum_{i=1}^{n} S_i}{\sum_{i=1}^{n} S_p} \qquad (2.12)$$

where S_i is the score for an individual forecast and S_p is the score for correct forecast. The summation is over n pairs of forecasts and observations. S_p will be determined on the sign of the numerator. If summation over S is negative, then S_p is the sum of the moduli of the worst possible scores, while if it is positive, S_p is the sum of the maximum possible scores. The significance of LEPS scores is calculated using 100 simulations of 77 random selected pairs of observed and forecasted categories.

2.3 Summary

The data and statistical methods used to analyse the data in this study, have been described. In the following chapters these methods will be applied to assess the predictability of monthly mean maximum temperature at various locations in South Africa. In the next chapter the method of singular value decomposition is used to determine which centres in the oceans are responsible for forecast skill of seasonal temperature over South Africa.

CHAPTER 3

ORIGINS OF SEASONAL FORECAST SKILL FOR SOUTH AFRICAN SURFACE-AIR TEMPERATURES

3.1 Introduction

The statistical techniques described in Chapter 2 are now used to investigate certain climatic features that relate global scale sea-surface temperatures (SST) to mean seasonal maximum surface-air temperature (T_x) over South Africa. In this chapter the method of singular value decomposition (SVD) is used to determine origins of forecast skill for mean seasonal maximum surface-air temperature of South Africa. An analysis of the space and time variation of the SST fields that give rise to forecast skill is conducted. First, the annual cycle of mean maximum monthly temperature is studied in order to define the different temperature seasons of South Africa, using principal component analysis (PCA). This is followed by an investigation of the origins of forecast skill for different seasons from global scale oceans.

3.2 Definition of Seasons

Principal component analysis is applied to long-term average monthly maximum temperature in order to study its seasonal variation over South Africa. Rule N (Preisendorfer, 1988) is used to select the significant modes of variance. It is found that the monthly temperature variations can be described in terms of a single principal component which accounts for more than 92% of the total variance, shown in Figure 3.1. The second principal component (PC2) declares less than 7% and all subsequent principal components together contribute to only 1% of the variability.

The correlation of the seasonal variation of T_x over South Africa with the first unrotated principal component is shown in Figure 3.2. Correlations of above 80% are evident across the entire field. The annual cycle of monthly mean maximum temperature over South Africa is therefore very well represented by the time series of the first unrotated principal component of temperature. From PC1 (Figure 3.1) the coldest three months over South Africa are June, July and August (JJA) (austral winter), while the warmest season (austral summer) is during

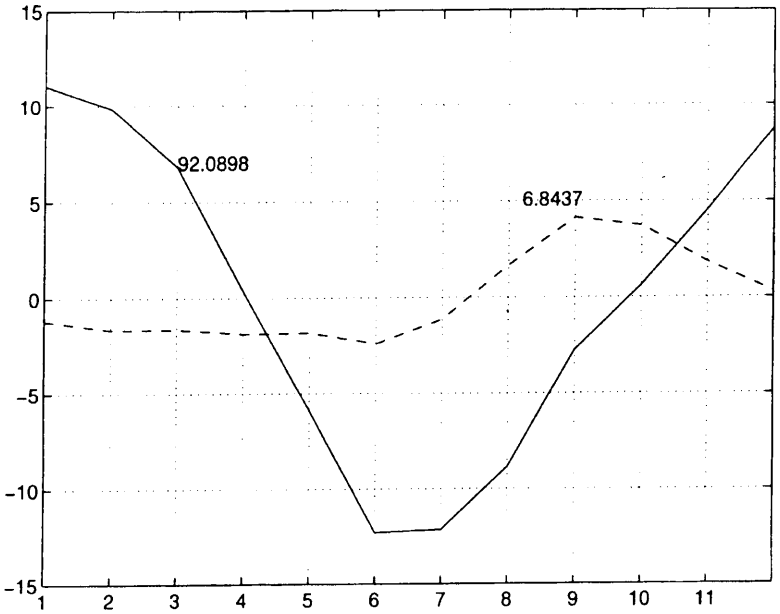

Figure 3.1 Principal component 1 (solid line) and 2 (broken line) of the seasonal variation of T_x over South Africa. The numbers indicate the explained variance in %.

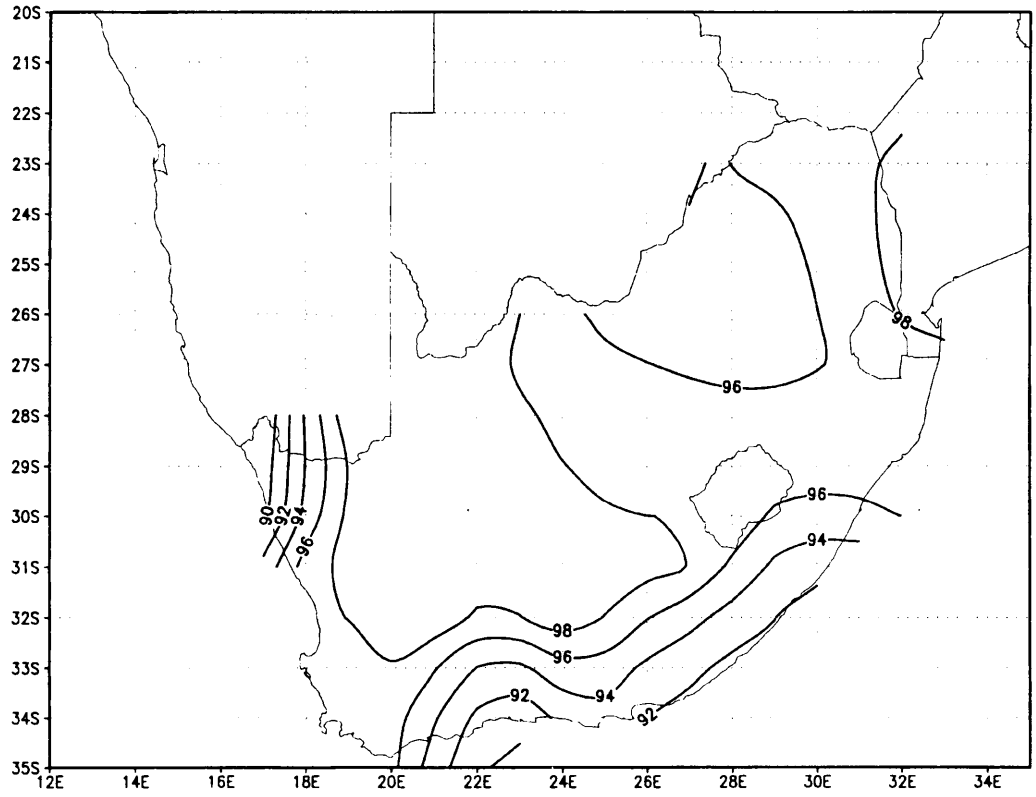

Figure 3.2 Correlation field of the first unrotated principal component of the seasonal variation of T_x over South Africa. All values are times 100.

December, January and February (DJF). Autumn will subsequently be defined as the 3-month period prior to winter (March, April and May - MAM) and spring the 3-month period that follows winter (September, October and November - SON). These correspond with the climatological seasons for the Southern Hemisphere. In this study the influence of global scale oceans on mean maximum temperature for these four seasons are investigated.

3.3 Origins of Forecast Skill

In this section the space-time analysis of the sea-surface temperature system that leads to high forecast skill in the four previously defined seasons, are investigated. The method of singular value decomposition (SVD) is used to seek for forcings from the ocean temperatures responsible for the forecast skill of seasonal mean maximum surface-air temperature in South Africa. SVD is chosen because of its ability to identify pairs of spatial patterns whose time series are characterized by maximum temporal covariance.

In this study, three consecutive 3-month mean SST fields (non-overlapping) for the period prior to the predictand season are used as predictors. For example, SST fields for MAM (2-season lag), JJA (1-season lag) and SON (0-season lag) are used to investigate the influence from the ocean areas on DJF mean maximum surface-air temperature over South Africa.

Table 3.1 depicts the different square covariance fractions (SCF) for the first three modes as obtained from the SVD runs. The strongest covariance from the first mode is found for autumn mean maximum temperature, followed by summer and winter with the weakest covariance found for spring. In all cases the second mode becomes more important on a longer lag, for example in summer the second mode's contribution to the variance between SST and T_x more than doubled from 0-season lag to 2-season lag as the variance explained by the first mode recedes.

Table 3.1 Squared covariance fractions (%) for Modes 1, 2 and 3 between different seasonal lags of sea-surface temperatures and the mean maximum temperature for climalogical seasons.

SVD Mode	2 Season Lag	1 Season Lag	0 Season Lag	Temperature Season
Mode 1	45.55	60.22	75.46	DJF
Mode 2	36.29	25.68	15.29	(summer)
Mode 3	3.37	2.90	1.67	
Mode 1	80.37	84.65	87.38	MAM
Mode 2	8.20	6.79	5.67	(autumn)
Mode 3	2.97	2.58	2.06	
Mode 1	60.31	69.25	74.35	JJA
Mode 2	15.59	13.20	9.21	(winter)
Mode 3	7.72	4.65	3.52	
Mode 1	37.5	50.03	52.71	SON
Mode 2	22.46	17.10	17.30	(spring)
Mode 3	17.98	13.94	13.33	

By investigating the temporal and spatial variability between the SST and T_x fields it is possible to draw some conclusions about the nature of the interactions between ocean and atmosphere that contribute to seasonal forecast skill of T_x over South Africa. In Figures 3.3 to 3.11 the heterogeneous SST map (top graph) for a specific season, lag and mode is shown. The middle graph depicts the expansion coefficient time series and the bottom graph shows the corresponding heterogeneous T_x map. The heterogeneous correlation maps indicate the strength of the association between the grid values of the SST (T_x) field and the expansion coefficient time series of the T_x (SST) field. Sign is pure convention.

To demonstrate the association between the SST and T_x, the spatial variation and the corresponding temporal variability (represented by the expansion coefficients) for the case of SVD mode 1 of summer surface-air temperature is discussed. Consider the heterogeneous maps of the first mode of summer T_x (Figure 3.3c) at 0-season SST lag (Figure 3.3a). For a particular mode, the correlations on the heterogeneous map indicate the association between the field values of the one field (i.e. SST) and the expansion coefficient of the other field (i.e T_x)

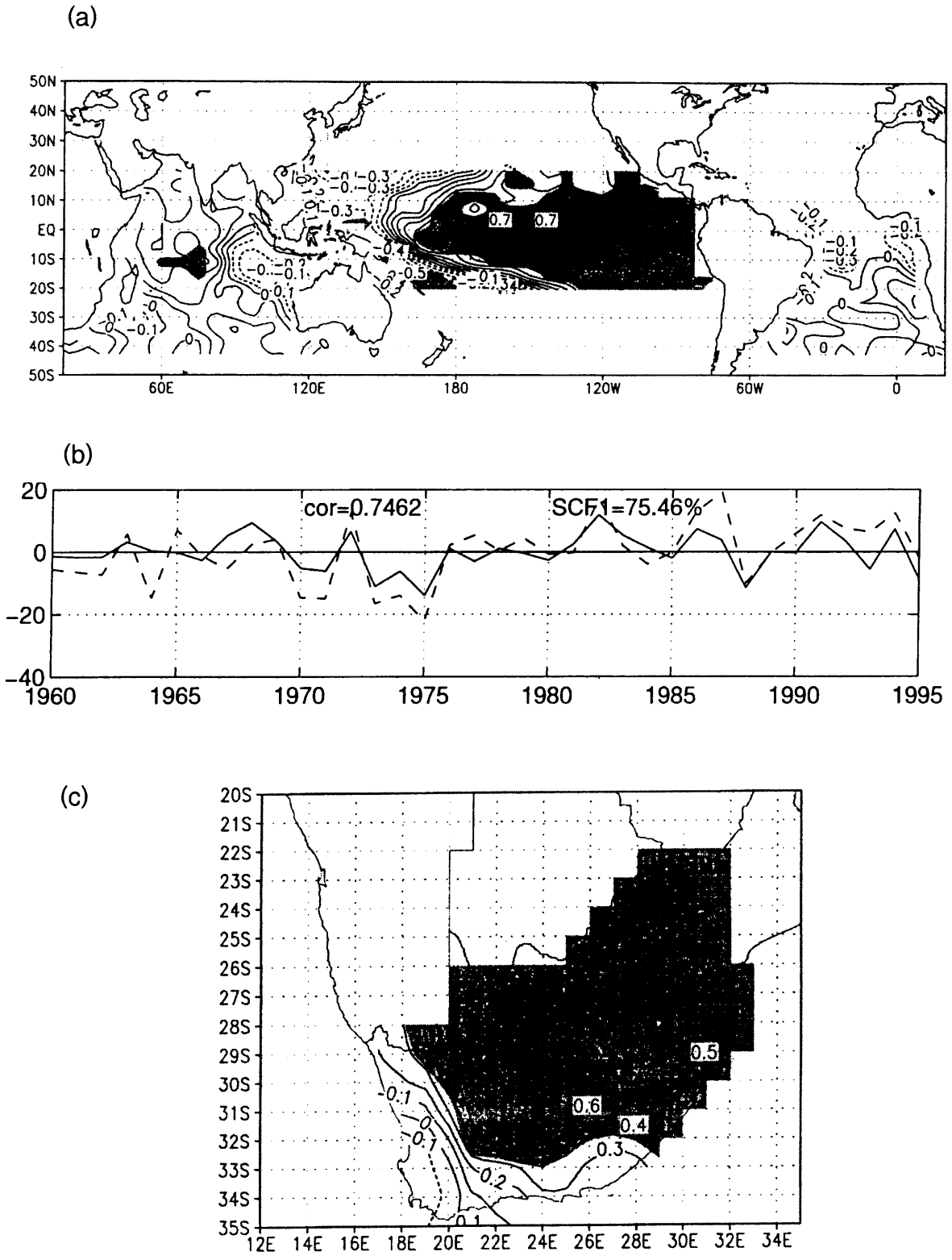

Figure 3.3 (a) Heterogeneous correlation map of mode 1 for the SON SST period influencing summer T_x. Areas significant at the 95% level are shaded.
(b) Time series of the SST (broken line) and T_x (solid line) singular vectors for mode 1 of DJF T_x using SON globalscale SSTs. "cor" indicate the correlation between the vectors and "SCF" the squared covariance fraction.
(c) The right field heterogeneous correlation map for SVD mode 1 of SON SSTs on summer temperature. Areas of significance above the 95% level are shaded.

and *vica versa*. From Figure 3.3a the sea-surface area of significance at a 0-season lag is found in the equatorial Pacific region mostly east of the date line, where the correlations between the SST field and the T_x expansion coefficient are statistically significant at the 95% level. The broken line in Figure 3.3b depicts the time series of the SST singular vector for mode 1. By applying Equation 2.3 for the La Niña episode of 1975/76, a negative score is implied. For the T_x field (Figure 3.3c) Equation 2.4 will result in a negative score for this mode. This implies that for a colder than normal equatorial Pacific sea-surface, colder than normal summer T_x is evident over South Africa. The opposite is true for the El Niño of 1982/83. Here a positive SST anomaly pattern corresponds with a positive T_x anomaly field, implying warmer than normal sea-surface temperature in the equatorial Pacific is associated with warmer than normal seasonal temperature in South Africa during summer months. The SVD modes for the four individual seasons will subsequently be discussed.

Summer - DJF

From the heterogeneous summer T_x maps of mode 1 (Figure 3.3c) over South Africa, the spatial distribution during summer is centred over the central and northeastern interior where the highest correlatons are found (Figure 3.3c). The left and right heterogeneous maps (Figures 3.3a and c) together with the temporal distribution of the first mode (Figure 3.3b) indicate that a cold equatorial Pacific Ocean will coincide with below average summer temperatures over the central and northeastern interior of South Africa. From the above discussion, the SST heterogeneous map of mode 1 shows an influence from the oceans which can be related to ENSO on the summer mean maximum temperature. Also, the time series of mode 1 (Figure 3.3b) shows distinct ENSO features such as the 1973/74 and 1975/76 La Niñas, the 1982/83 El Niño and the 1988/89 La Niña (Schulze, 1989).

The second mode becomes more important as one recedes further from the summer maximum temperature season (Table 3.1). The ocean signal during summer months as revealed by mode 2 indicates a SST trend which comes largely from the Indian, and the southern Atlantic oceans. With longer lag (two seasons) the western Pacific ocean (excluding the equatorial region) becomes also significant (Figure 3.4a). From mode 2, negative sea-surface temperature anomalies in the significant ocean areas will coincide with positive T_x anomalies over the significant west coast areas of South Africa (Figure 3.4c) during summer.

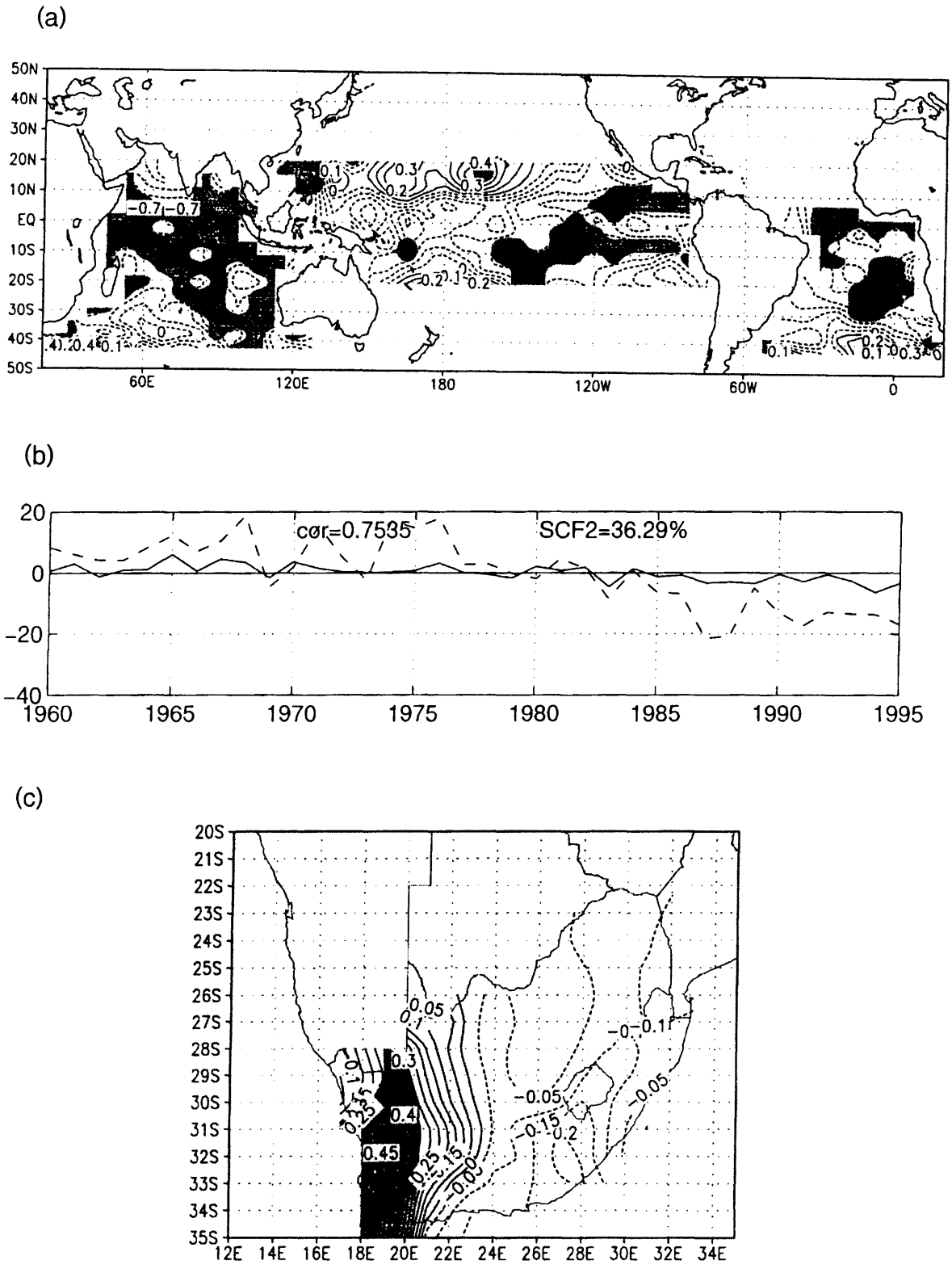

Figure 3.4 As for Figure 3.3, but for mode 2 of MAM SSTs.

Autumn - MAM

The leading SVD mode for autumn explains more than 80% of the squared covariance between the SST and surface-air temperature fields at all lags. The heterogeneous and homogeneous correlation patterns for the first mode at 0-season lag is shown in Figure 3.5a. The strongest centres of action are over the equatorial Pacific and Indian oceans. Once again the ENSO related signal is evident from the time series (Figure 3.5b) of the first SVD mode. The corresponding right correlation fields (Figure 3.5c) show the main influence from these sea-areas over South Africa. Investigation of the left and right heterogeneous maps and the corresponding time series reveals that an anomalously warm equatorial ocean results in above average mean maximum temperatures during autumn, and *visa versa*.

The second SVD mode (Table 3.1) contributes much less to the squared covariance, but shows small significant areas in the southern Atlantic, southern Indian and Equatorial Pacific just north of Australia (Figure 3.6a). Over the continent the corresponding spatial distribution shows areas of significance mainly along the west coast (Figure 3.6c). This is very similar to what was found for the second mode of summer temperature.

Winter - JJA

The signal from the first mode for winter is weaker than for autumn. From the heterogeneous (Figure 3.7a) map only small areas of the south Atlantic, south Indian and south equatorial Pacific oceans correlate significantly with the expansion coefficient score of wintertime T_x. From the time series (Figure 3.7b) an ENSO signal together with a trend in ocean temperatures are seen. The T_x heterogeneous map for mode 1 (Figure 3.7c) shows that the signal is reflected over the interior of South Africa. By applying equations 2.3 and 2.4 from the previous chapter, anomalous warm temperatures in the significant sea areas will result in anomalously warm winter temperatures over the interior of South Africa, and cold SSTs will result in anomalously cold winter temperatures on a short lead.

The SST and T_x maps for the second SVD mode is shown in Figure 3.8. Only a few isolated ocean areas of significance are found (Figure 3.8a), but the corresponding maximum-temperature correlation field (Figure 3.8c) shows a distinct dipole between the northeastern and western parts of South Africa. The opposite signs of these two centres indicate that different reaction due to the SST field are expected in these regions.

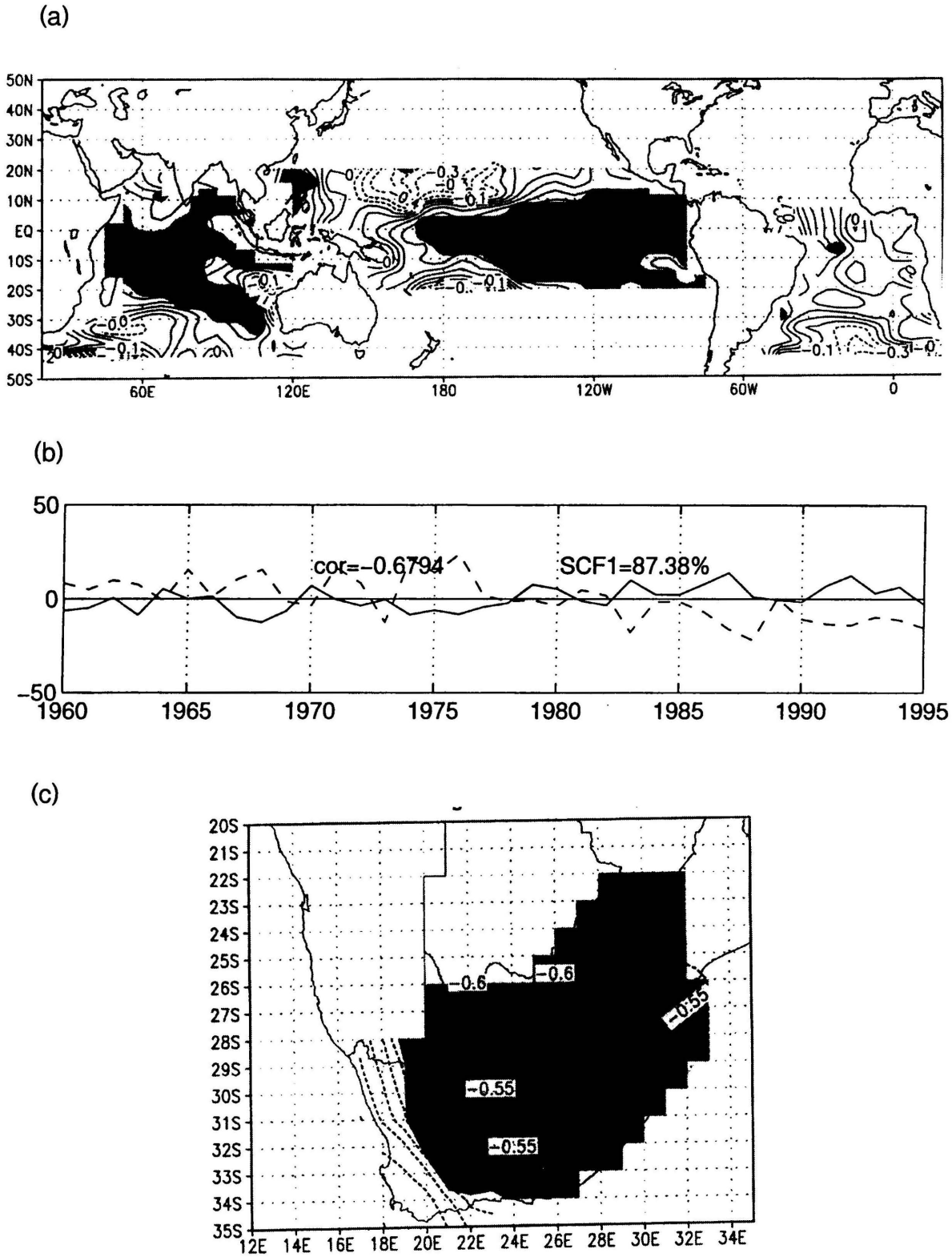

Figure 3.5 As for Figure 3.3, but for mode 1 of DJF SSTs influencing autumn T_x.

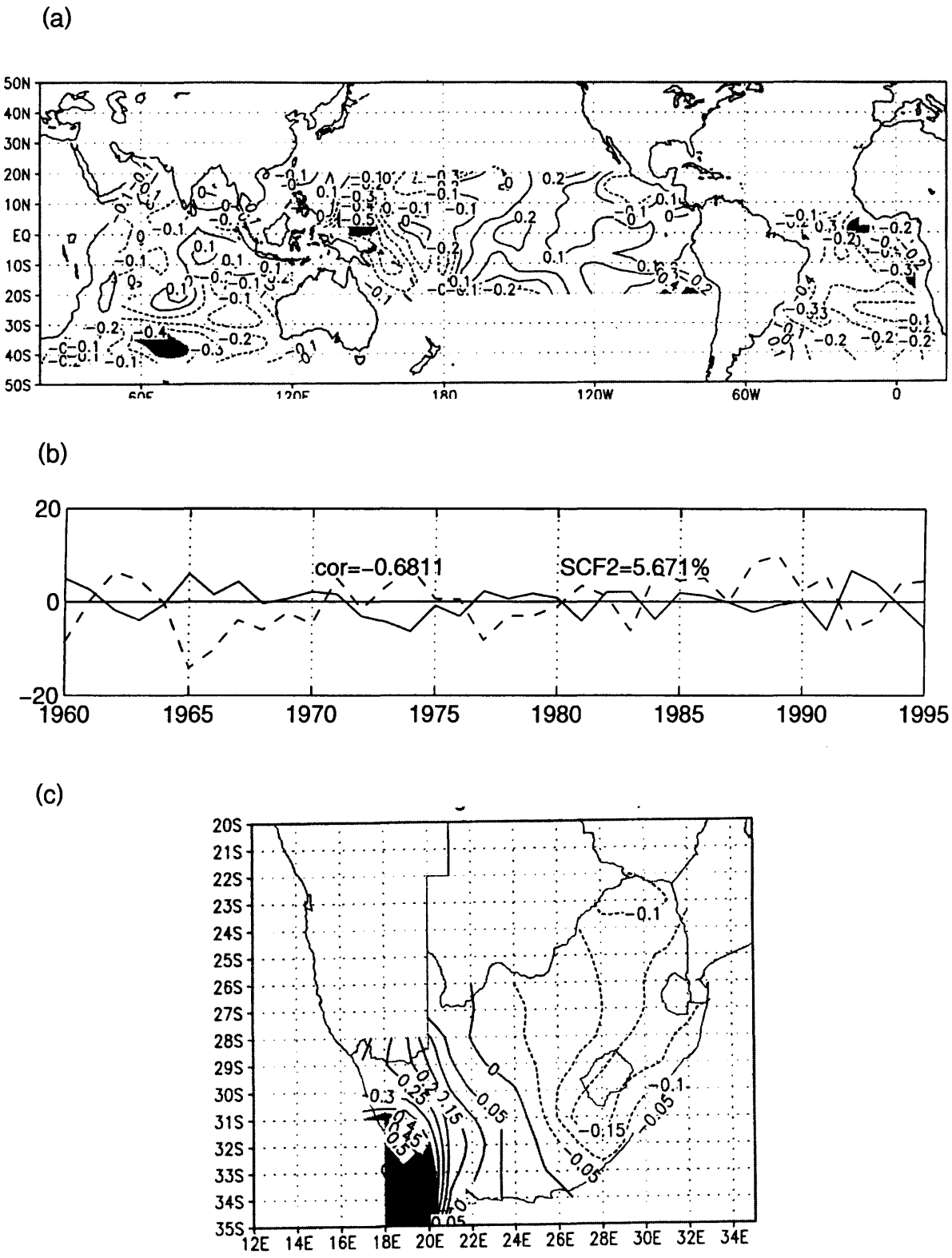

Figure 3.6 As for Figure 3.3, but for mode 2 of DJF SSTs influencing autumn T_x.

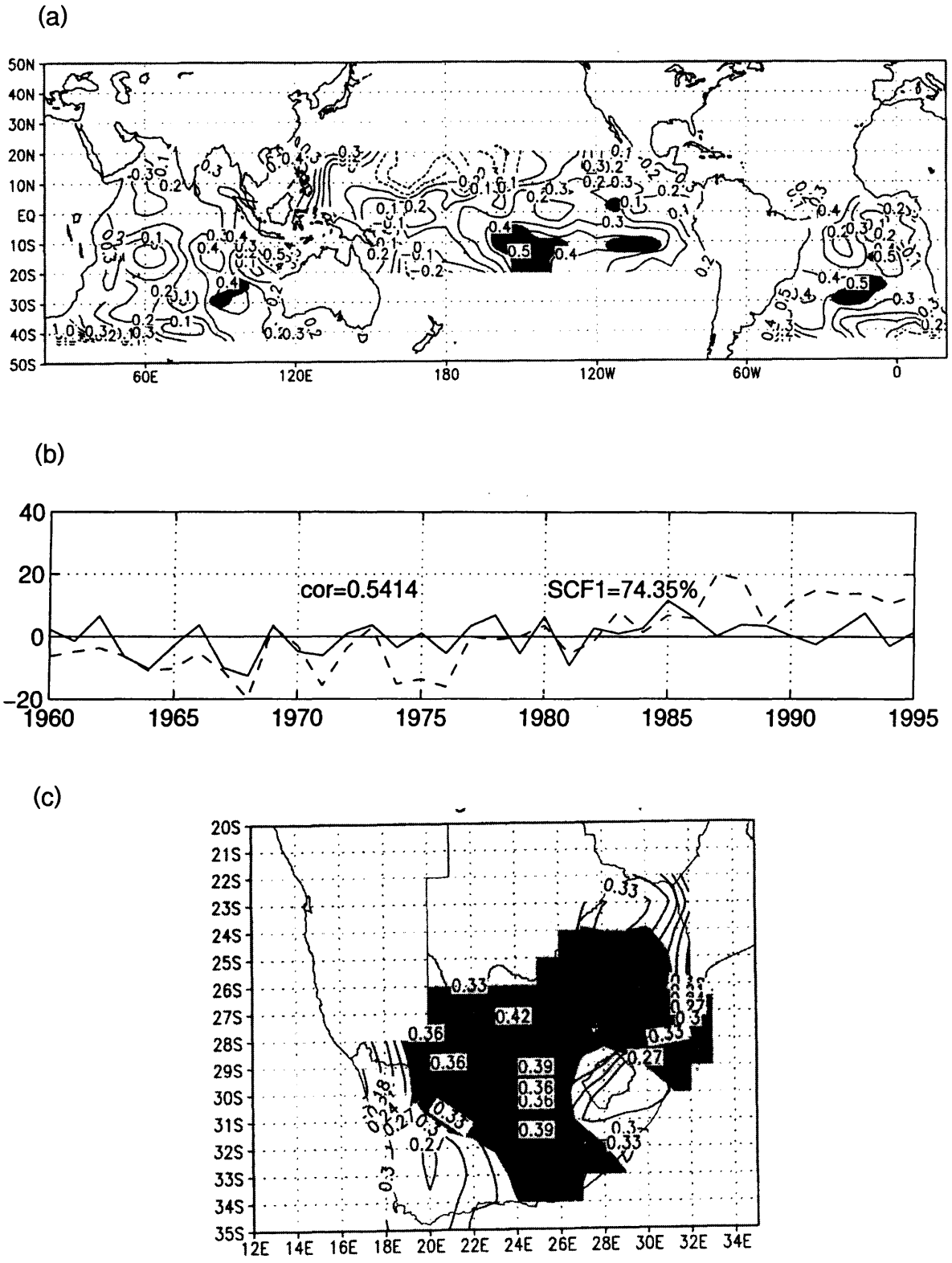

Figure 3.7 As for Figure 3.3, but for mode 1 of MAM SSTs influencing winter T_x.

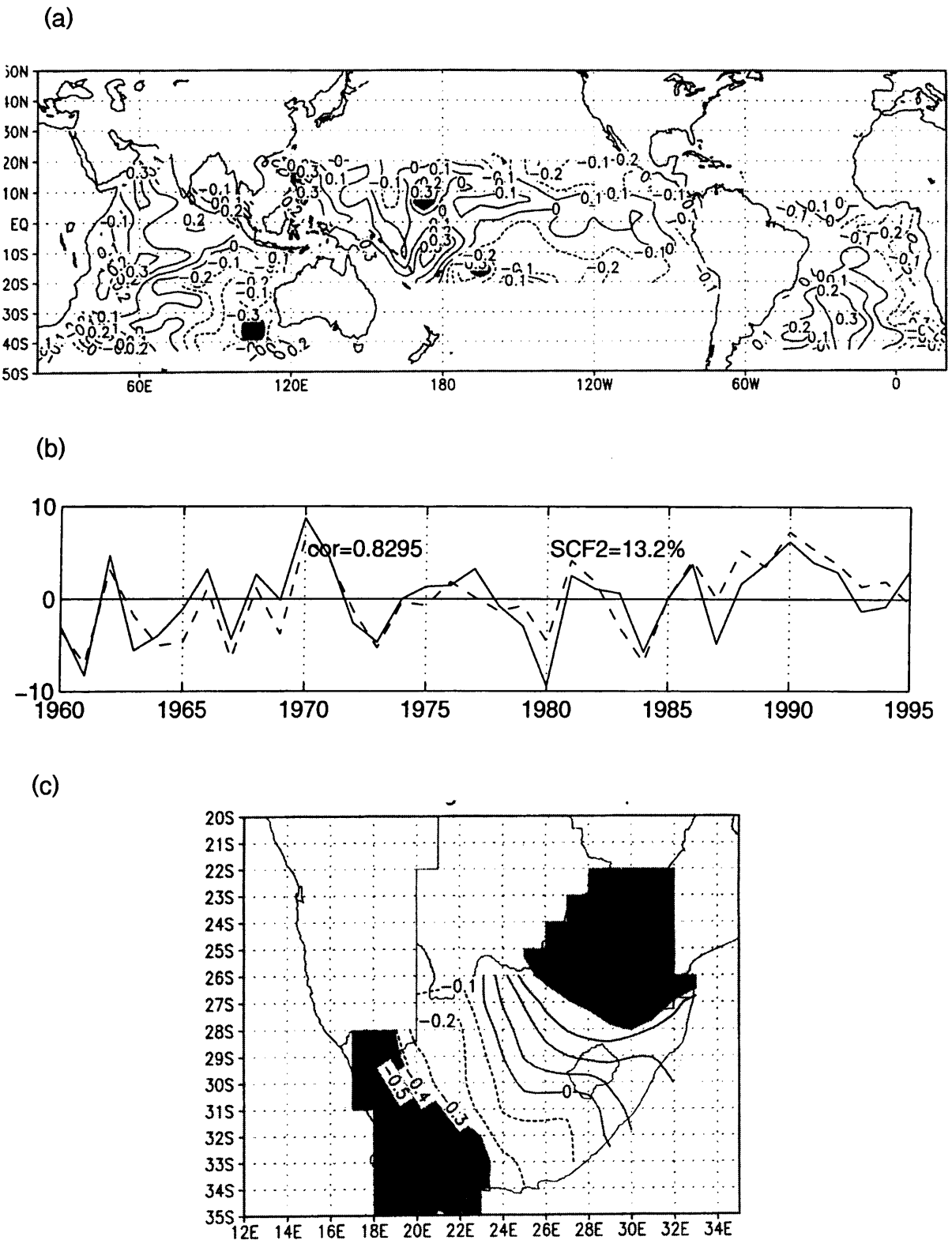

Figure 3.8 As for Figure 3.3, but for mode 2 of DJF SSTs influencing winter T_x.

By investigating the time series of mode 2 (Figure 3.8b) together with the left and right heterogeneous maps (Figures 3.8a and c), it may be concluded that above-normal SSTs in the significant ocean regions will result in anomalously cold mean maximum temperatures over the northeastern parts of South Africa, and anomalously warm mean maximum temperatures over the western parts of the country, and *vice versa*.

Spring - SON

The weakest seasonal temperature associations with global scale SSTs are during spring. Slightly over half of the covariance is explained by the first singular mode (Figure 3.9b). On the SST heterogeneous map (Figure 3.9a) a significant area in approximately the Niño-3 (5°N to 5°S; 90 to 150 °W) region is shown. Also, small areas in the western Indian and southern Atlantic oceans are significant. From the time series (Figure 3.9b) a trend in SSTs is evident. The corresponding T_x heterogeneous field shows the influence of this ocean area to be over the western and southwestern parts of South Africa (Figure 3.9c). From these maps, considering also the expansion coefficient score (Figure 3.9b) it may be concluded that anomalously cold (warm) SSTs result in anomalously cold (warm) spring temperatures over the southwestern and western regions of South Africa.

The heterogeneous map for mode 2 of the 0-season lag SST field (Figure 3.10) shows no conclusive area of significance, while the heterogeneous spatial map of T_x (Figure 3.10c) shows a significant region over the Lesotho Highland and eastern Free State regions. From the time series a trend in ocean temperatures is once again well defined (Figure 3.10b). No conclusion could be drawn from these maps because of the poor relation found in Figure 3.10a.

Because the first two modes explain a relatively small amount of the covariance, three modes are considered for spring. It is interesting to note that the spatial pattern of the right field (T_x) of mode 3 (Figure 3.11c) resembles similar features as for the second mode of all other seasons, namely the correlation dipole between northeastern and western parts of South Africa. The ocean signal in the case of mode 3 for spring comes from the eastern Indian and western Pacific oceans as depicted in Figure 3.11a where a 50-year cycle is suggested.

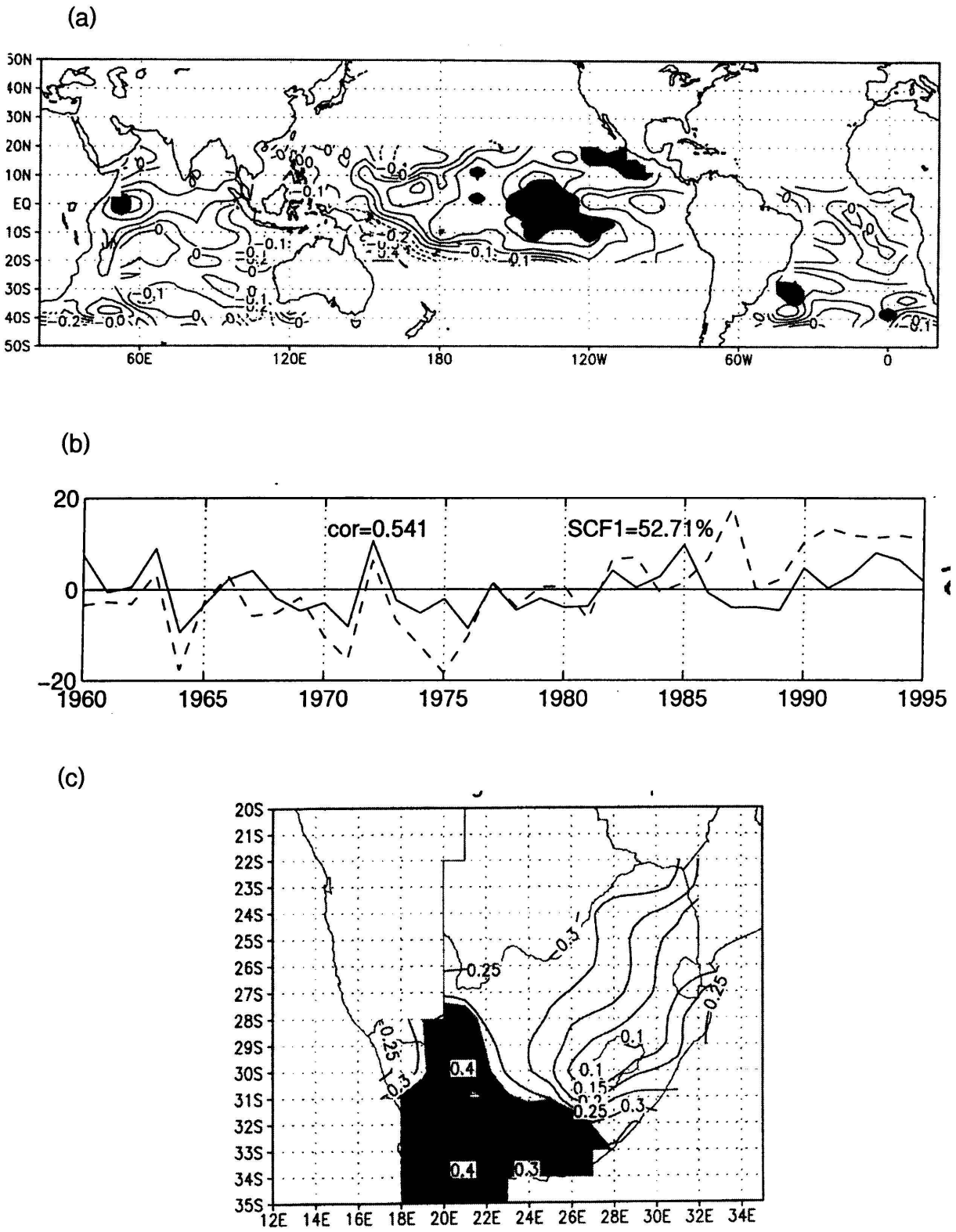

Figure 3.9 As for Figure 3.3, but for mode 1 JJA SSTs influencing spring T_x.

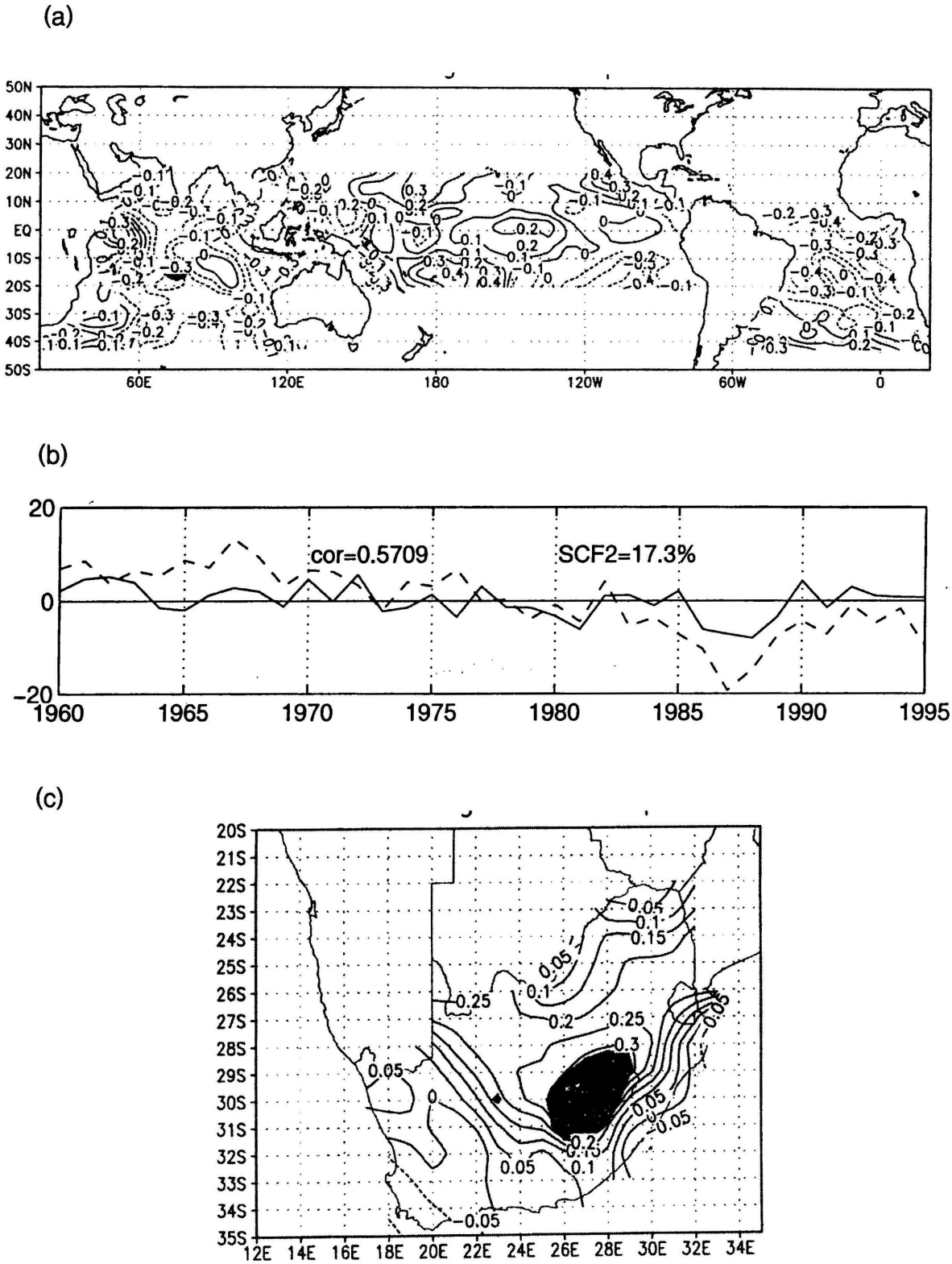

Figure 3.10 As for Figure 3.3, but for mode 2 of JJA SSTs influencing spring T_x.

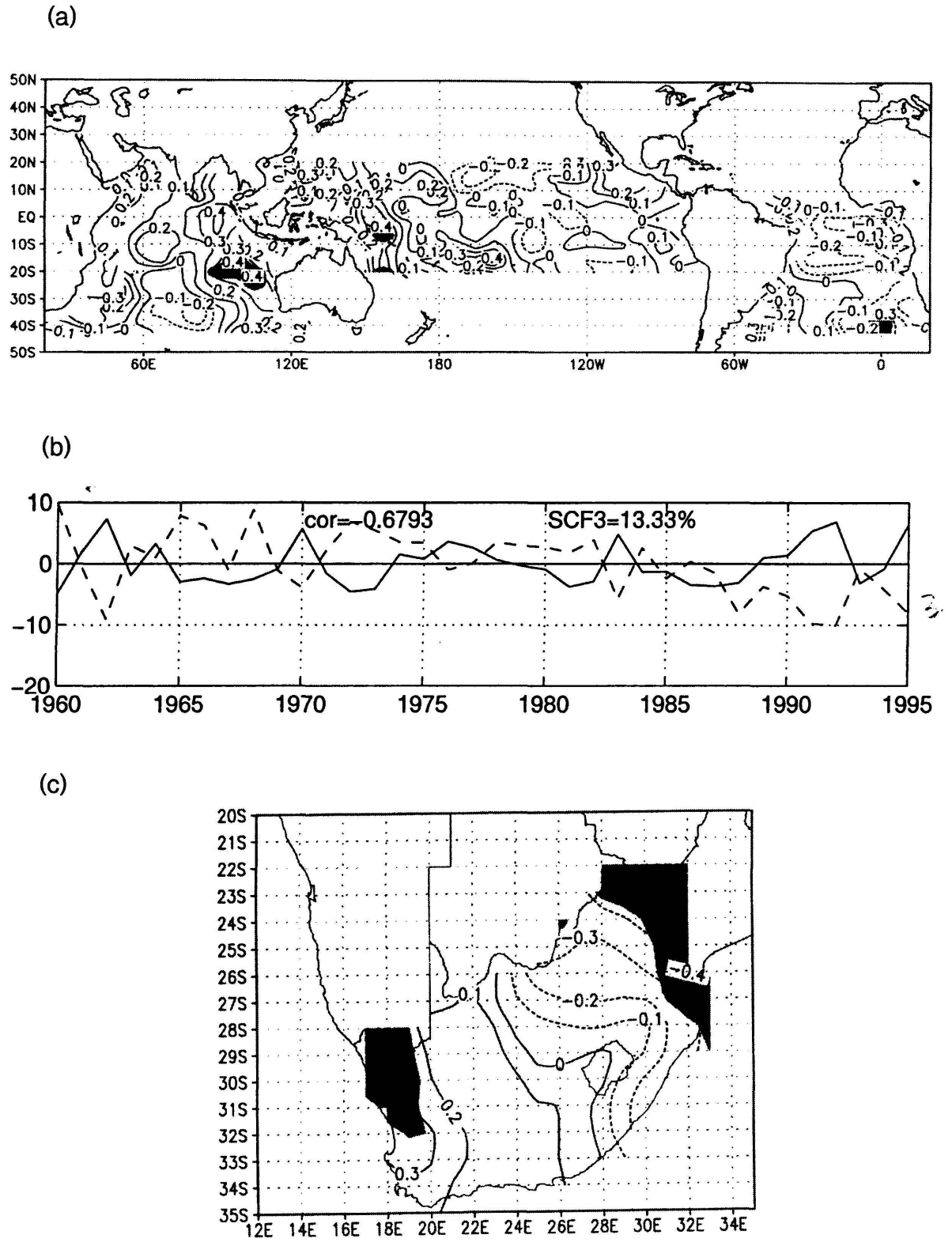

Figure 3.11 As for Figure 3.3, but for mode 3 of JJA SSTs influencing spring T_x.

3.4 Summary

The results of section 3.3 give a picture of the space-time analysis of the SST climate fields that leads to predictive skill of seasonal mean maximum temperature over South Africa. An analysis of the centres of action in the SST field for the different seasons suggests that ENSO-related features resemble an important influence on the seasonal temperature of South Africa especially during summer and autumn. The relationship is so that warm (cold) equatorial Pacific SSTs coincide with warm (cold) mean seasonal temperatures over the significant areas over the country. The spatial distribution of the right field (temperature over South Africa) consistently shows the influence of first mode SSTs over the central interior and eastern half of South Africa.

Furthermore, the ocean areas adjacent to South Africa capture a large portion of the remaining covariance that is mainly associated with the long-term warming trend in the tropics and mid-latitude southern oceans. The second mode T_x heterogeneous maps suggest a temperature dipole between northeastern regions and western areas for all seasons except spring, where this feature is only evident for the third mode. Rotation of the weight vectors will result in patterns that are easier to interpret and reduce the possibility of Buell patterns occurring. The T_x anomaly over the western areas corresponds to the significant SST anomaly, while the opposite T_x anomaly is found over the eastern parts. In other words, cold (warm) SSTs in the significant ocean areas will result in warm (cold) seasonal temperatures over the western parts, and cold (warm) seasonal temperatures over the northeastern regions. The second mode during spring shows a significant region over the Lesotho Drakensberg areas.

It can be concluded that global scale SSTs should contribute to the predictability of seasonal temperature over South Africa since large spatial regions of significant correlations exists, especially during summer and autumn months. The most important SST modes are related to ENSO and a long-term global warming trend in the oceans. In the next chapter the atmospheric response to the sea-surface forcing is analysed with specific reference to the first SST mode and corresponding atmospheric circulation over South Africa.

CHAPTER 4

ATMOSPHERIC CIRCULATION

4.1 Introduction

It was shown in Chapter 3 that the ENSO forcing on temperature over South Africa is strong and accounts for the largest amount of variance in all seasons, especially during summer and autumn. In Chapter 3 the focus was on the forcing from the ocean temperatures. The atmospheric component of ENSO, namely the Southern Oscillation (SO) has effects globally although its main centres of action are in the tropics (Trenberth, 1991). Bjerknes (1969) was the first to describe the dynamic and thermodynamic coupling between the ocean and atmosphere that dominates interannual climate variability over much of the tropics and deep into the extra tropics. In this chapter the changes in atmospheric circulation over South Africa during ENSO events are described with specific reference to the warm event of 1982/83 and the cold event of 1988/89.

4.2 Southern Oscillation

The Southern Oscillation (SO) is mainly a pressure dipole that fluctuates at two centres which are thousands of kilometres apart. Sir Gilbert Walker first named these fluctuations the Southern Oscillation (Walker, 1923, 1924, 1928). It was then established that the SO involves far more than just a seesaw in the surface pressure difference across the Pacific Ocean. The association of the SO with major changes in meteorological patterns across the globe was recognise early this century (Walker and Bliss, 1930, 1932, 1937).

The SO has since been studied extensively, and it is well known that the low phase of the SO is associated with anomalously warm central Pacific SSTs (El Niño), while the high phase of the SO occurs in conjunction with cold events (La Niña). However, it is important to note that there is not a one-to-one correspondence between the occurrence of SO events and El Niño (or La Niña) events (Trenberth and Shea, 1987). Investigations on links between ENSO and midlatitude temperature and rainfall were performed by Rasmusson and Carpenter (1982), Shukla and Paolino (1983), Kousky *et al.* (1984) and others. The principal factor is that large scale atmospheric motion in the tropics on time scales of weeks to months and longer,

correspond to direct thermal circulations (Philander, 1990). The SO acts as a perturbation to these direct thermal circulations and is associated with fluctuations in the intensity and positions of regions of rising moist air. The factors that influence the interannual movements of convective zones (variations in SST patterns and in the heating of continents) also influence the seasonal movement of convective zones. The SO and the seasonal cycle of convective zones therefore have much in common (Philander, 1990).

The SO involves interannual variations in the direct thermal circulation of the tropics, but also affects the atmospheric circulation outside the tropics in a more indirect manner. These effects are most pronounced during the mature phase of El Niño when an anticyclonic couplet in the upper-air wind field develops in the upper troposphere over the central Pacific Ocean where the anomalous heating of the ocean is a maximum (Philander, 1990). The couplet is associated with a strengthening of the Hadley circulation (mean zonal circulation) and with the appearance of upper-level easterly wind anomalies near the equator. On the poleward flanks of the couplet, the subtropical jet streams are intensified and displaced equatorward, possibly causing the exceptional rainfall and temperature disturbance around the world (Berlage, 1966; Horel *et al.*, 1986).

4.3 Surface-air Temperature Patterns Associated with the Southern Oscillation

While most of the relationships between the SO and air temperatures in tropical regions can be associated with either shifts in convection zones or to the direct influence of changes in SSTs, SO-temperature patterns in the extra tropics are probably related to shifts in the large-scale flow pattern (Rasmusson and Wallace, 1983). Halpert and Ropelewski (1992) presented results to illustrate that SO-temperature relationships are global in nature. Figure 4.1 illustrates the principal core areas with significant SO-temperature relationships. The strongest SO-temperature relationships occur in the tropics where the general increase or decrease in surface temperature throughout the global tropics is a delayed response to the warming or cooling of equatorial SSTs. The SO-temperature relationships outside the tropics are more complex than the tropical responses since they are the result of tropical forcing of circulation patterns (Halpert and Ropelewski, 1992).

a)

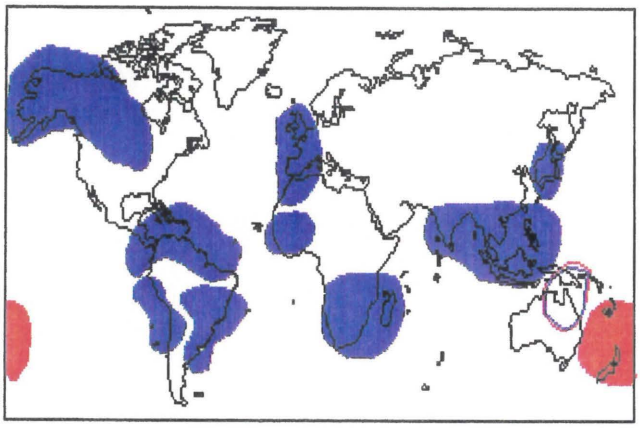

b)

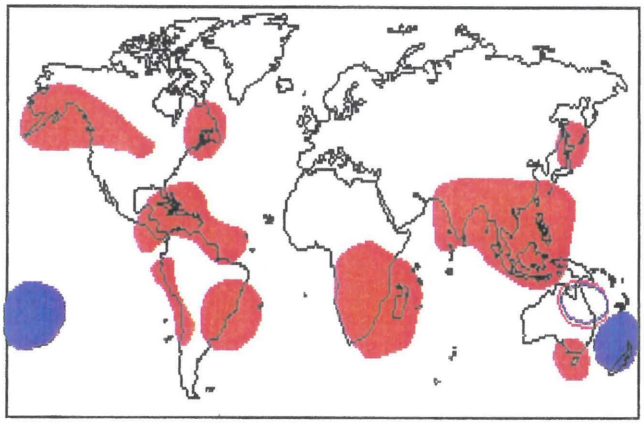

Figure 4.1 Schematic representation of the principal a) cold and b) warm ENSO event temperature relations (after Halpert and Ropelewski, 1992). Blue indicates anomalously cold temperatures and red, anomalously warm temperatures.

Seasonal temperature anomalies over southeast Africa are generally of the same sign as equatorial Pacific SST anomalies during an ENSO event. The temperature response over southeast Africa during the cold event years appears to begin earlier (August) than during warm event (October) years (Halpert and Ropelewski, 1992).

4.4 Circulation over South Africa during ENSO events

The Southern Oscillation and resulting global responses are well described in the literature. It is now important to investigate the mean circulation features over South Africa that occurs as a result of the warm and cooling of equatorial Pacific sea-surface temperatures, and the accompanying Southern Oscillation. In this section the difference between mean seasonal circulation features during the El Niño of 1982/83 and the La Niña of 1988/89 is discussed as an example. Although it is only one example it will give an indication of the circulation differences associated with these events. Since the strongest ENSO forcing on temperature over South Africa occurs during austral summer and autumn months (refer Chapter 3), these two periods are compared

El Niño 1982/83

The exceptional warm event of 1982/83 resulted in below-normal cloud cover (and rainfall) and consequently anomalously warm surface-air temperatures over most of South Africa. The south-western Cape coastal belt experienced near-normal to mostly below-normal temperatures where above-normal rainfall occurred during this season.

1. Summer (DJF)

An upper air high pressure system is indicated in Figure 4.2a over Namibia with an influx of subtropical air from the west. Positive 500 hPa geopotential height (gpm) anomalies occurred over the subcontinent during this period (Figure 4.2b). A surface trough was situated in the mean across Botswana and the central parts of South Africa during the summer months (Figure 4.3a). The weak surface high pressure to the east of the through resulted in reduced flow of moist air from the east over these areas. From the anomaly field negative surface pressure anomalies (thus a weaker than normal high pressure system) is evident over the eastern parts of the subcontinent with positive anomalies (deeper than normal high pressure) over the central an western regions (Figure 4.3b).

2. Autumn (MAM)

Positive 500 hPa gpm anomalies occurred over the subcontinent during autumn months following the 1982/83 El Niño event (Figure 4.4b). An upper troposphere through was situated

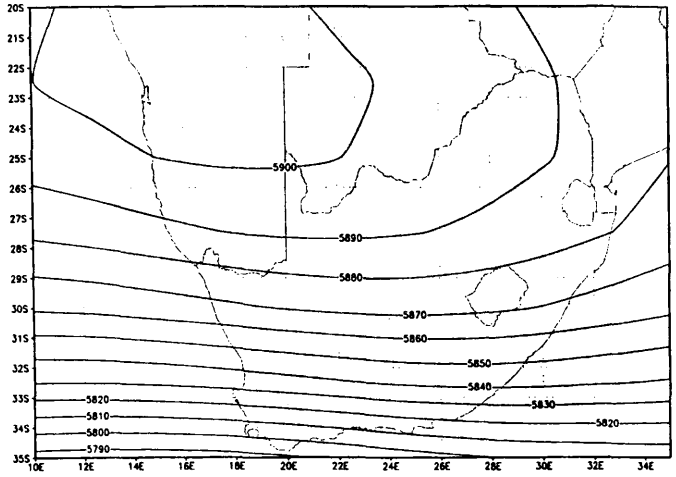

Figure 4.2a December-January-February 1982/83 mean 500 hPa gpm contours over South Africa.

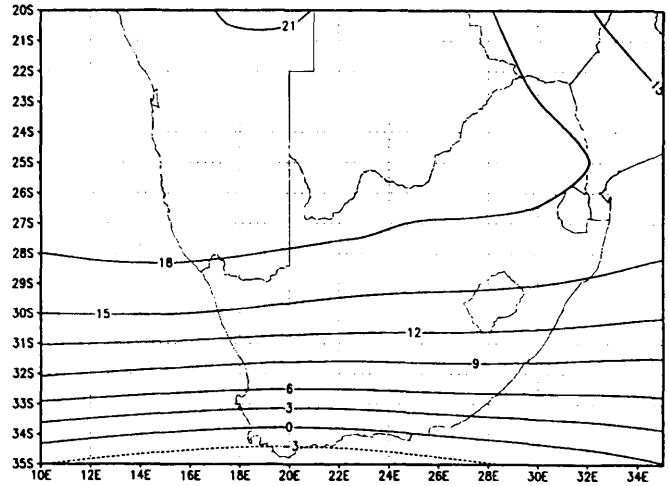

Figure 4.2b December-January-February 1982/83 mean 500 hPa gpm anomalies.

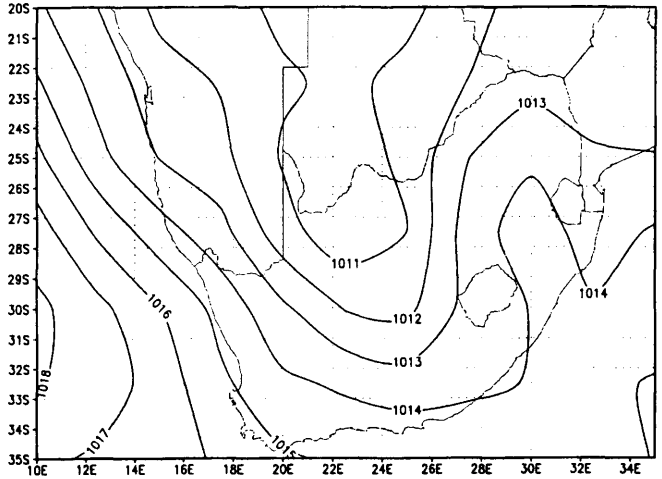

Figure 4.3a December-January-February 1982/83 mean sea-level pressure over South Africa.

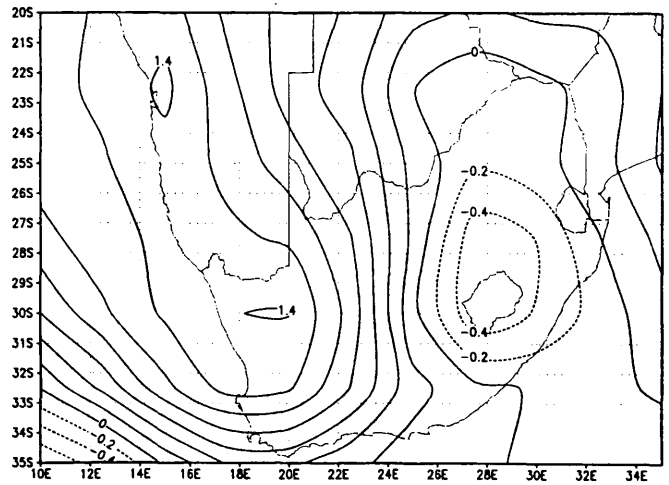

Figure 4.3b December-January-February 1982/83 mean sea-level pressure anomalies.

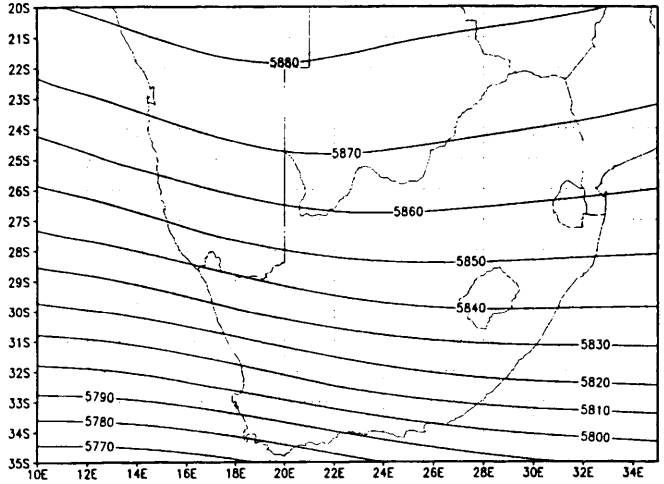

Figure 4.4a March-April-May 1983 mean 500 hPa gpm contours over South Africa.

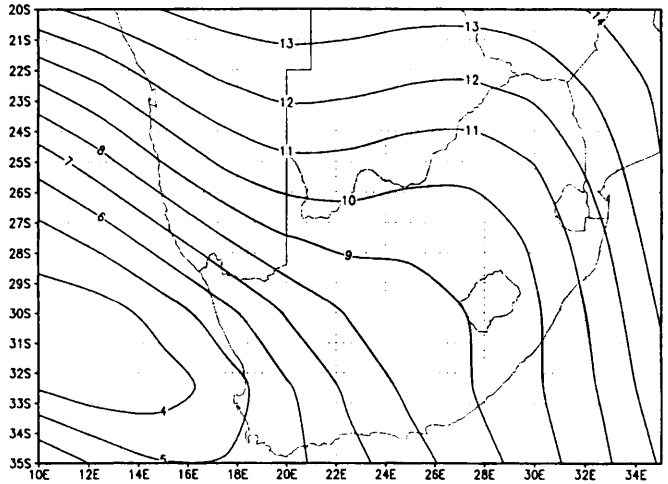

Figure 4.4b Marc-April-May 1983 mean 500 hPa gpm anomalies.

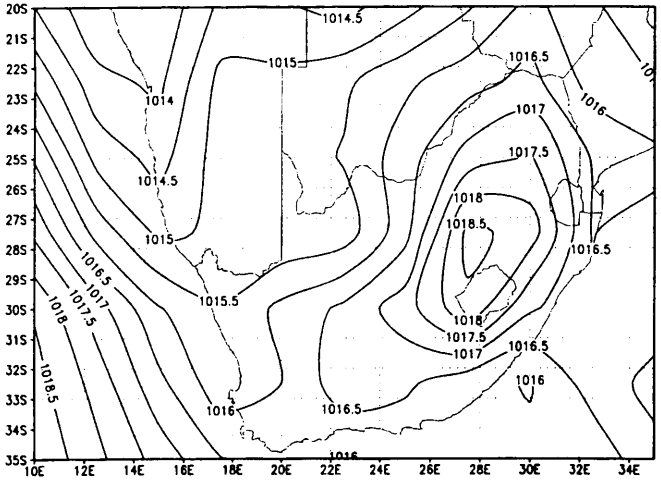

Figure 4.5a March-April-May 1983 mean sea-level pressure over South Africa.

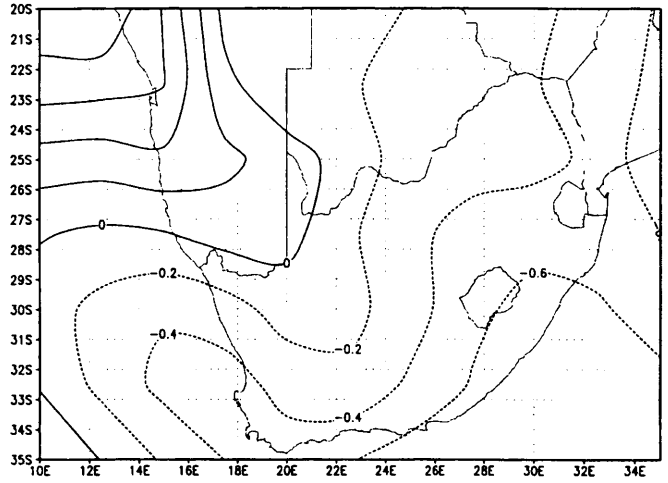

Figure 4.5b March-April-May 1983 mean sea-level pressure anomalies.

west of the subcontinent (Figure 4.4a). From Figure 4.5a a surface trough was evident over the west coast, with a high pressure area occurring over the eastern parts of the subcontinent. On the surface (Figure 4.5b) negative SLP anomalies occurred over most of the area indicating a weaker than normal high pressure.

La Niña 1988/89

During this cold event high rainfall was received over South Africa and below-normal temperatures occurred due to the large amount of cloud cover experienced.

1. Summer (DJF)

The upper-air high pressure is situated over the northeastern parts with an upper-air trough west of the subcontinent (Figure 4.6a) indicating the presence of a west coast upper trough. Negative 500 hPa gpm anomalies are evident over the whole region (Figure 4.6b) indicating that upper-air pressure is low.

The mean circulation during the summer months indicates a surface high pressure system situated over the eastern parts of South Africa (Figure 4.7a) which caused an influx of moist air from the southeast from the Indian ocean. A well developed surface trough can be seen over Botswana and the central parts of South Africa. An area of positive pressure anomalies is evident over the eastern parts and negative anomalies over the western regions of the subcontinent (Figure 4.7b).

2. Autumn (MAM)

Figure 4.8a indicates the mean upper-air (500 hPa) circulation during the autumn months following the La Niña period. Negative anomalies are found across the entire region (Figure 4.8b) indicating upper-air low pressure.

The mean surface pressure map indicates an area of high pressure over the eastern parts and a surface trough over the west coast (Figure 4.9a). On the surface negative pressure anomalies are found over the northwestern parts and positive anomalies over the central and eastern regions of southern Africa (Figure 4.9b).

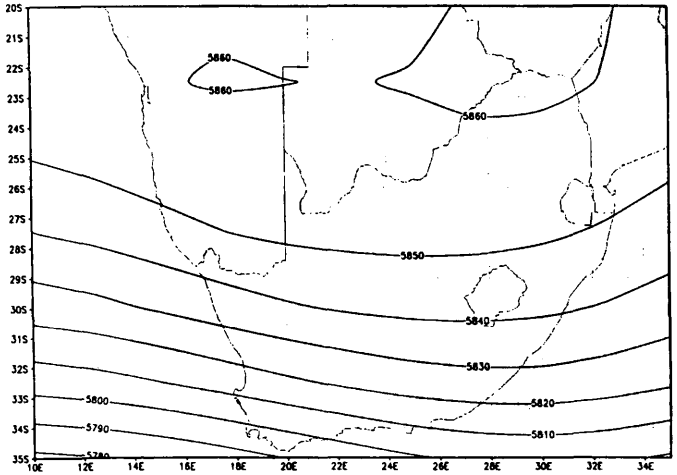

Figure 4.6a December-January-February 1988/89 mean 500 hPa gpm contours over South Africa.

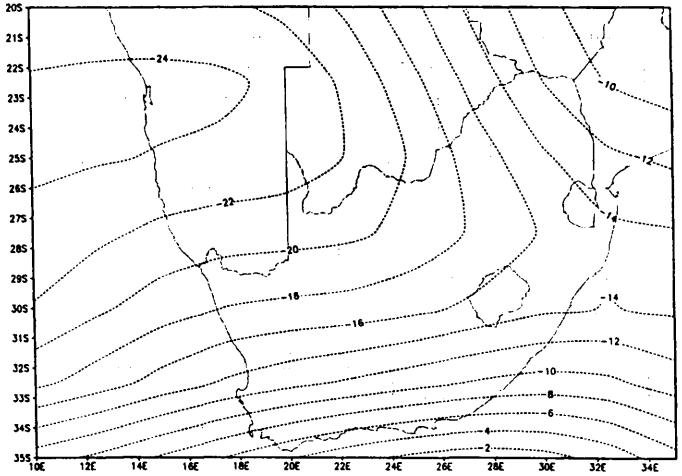

Figure 4.6b December-January-February 1988/89 mean 500 hPa gpm anomalies.

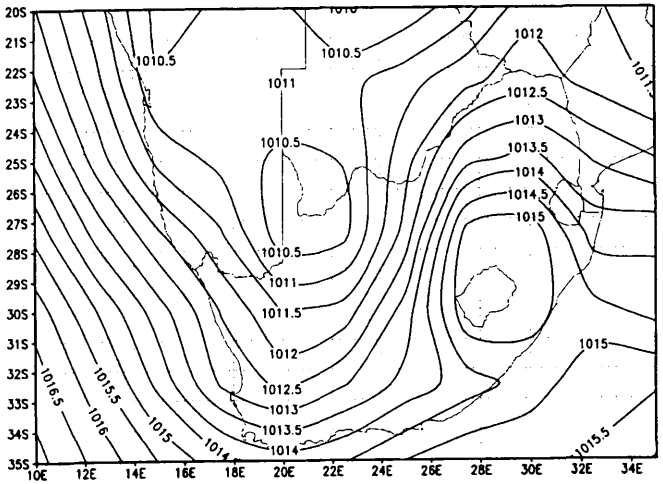

Figure 4.7a December-January-February 1988/89 mean sea-level pressure over South Africa.

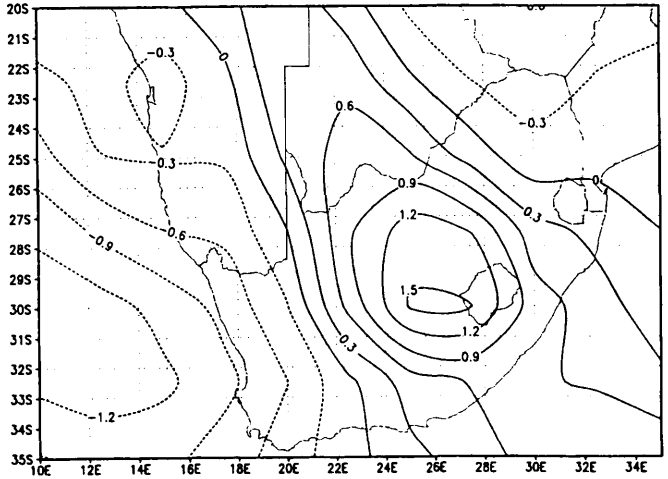

Figure 4.7b December-January-February 1988/89 mean sea-level pressure anomalies.

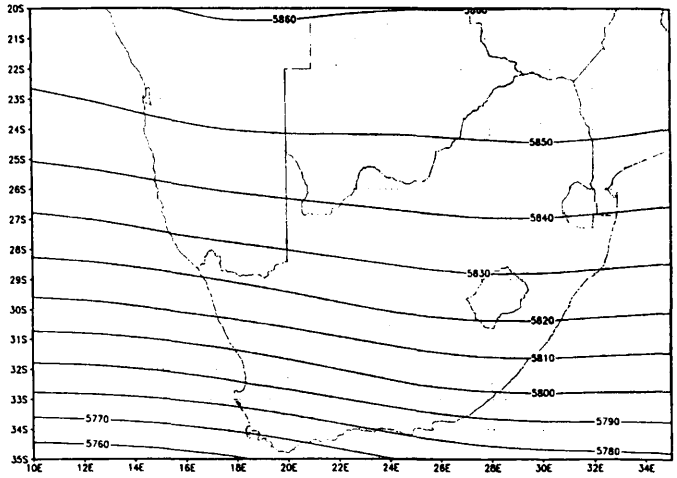

Figure 4.8a March-April-May 1989 mean 500 hPa gpm contours over South Africa.

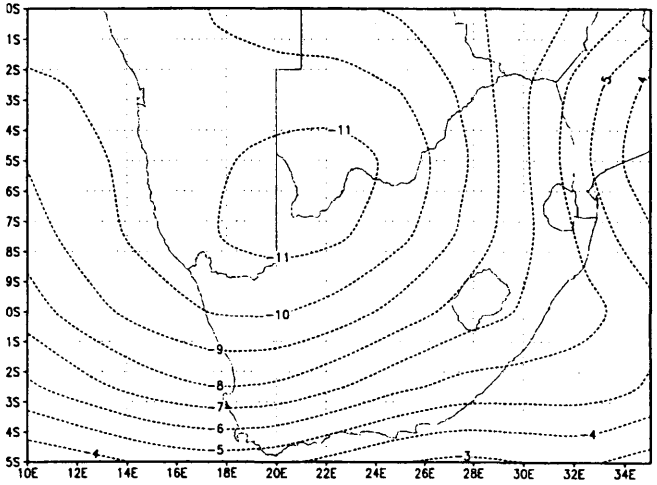

gure 4.8b Marc-April-May 1989 mean 500 hPa gpm anomalies.

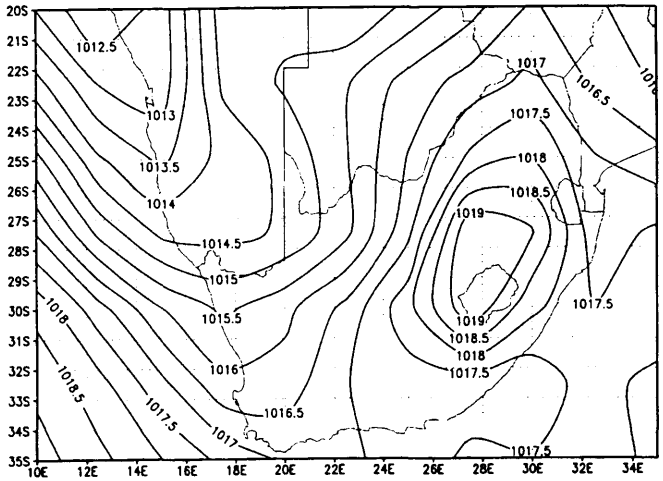

Figure 4.9a March-April-May 1989 mean sea-level pressure over South Africa.

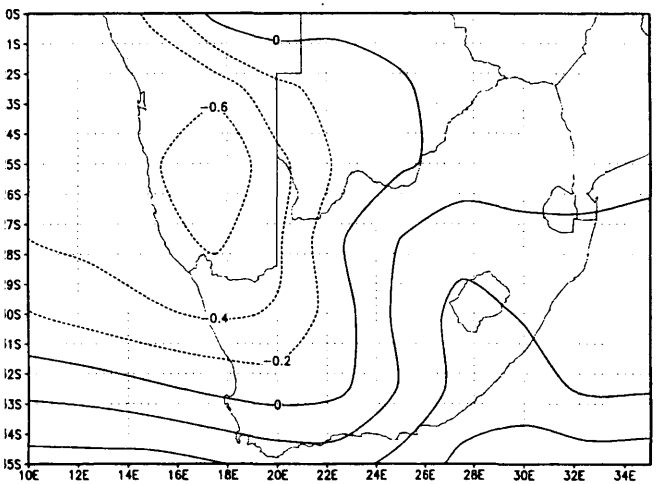

igure 4.9b March-April-May 1983 mean sea-level pressure anomalies.

Discussion

Tables 4.1 and 4.2 summarize the main circulation features occurring during different phases of the ENSO phenomenon with specific reference to the 1982/83 El Niño and the 1988/89 La Niña.

Table 4.1. Difference between the mean circulation features in summer months during the El Niño event of 1982/83 and the La Niña of 1988/89.

DJF	1982/83	1988/89
500 hPa	• The upper-air high pressure system is situated over the western parts of southern Africa. • A stronger geopotential gradient and a deeper upper-air high pressure system is indicated causing an increase in upper-air westerlies. • Positive 500 hPa gpm anomalies over the entire subcontinent.	• The upper-air high pressure system is situated over the eastern parts of southern Africa. • A weaker geopotential gradient and a weaker upper-air high pressure system occurred causing a decrease in upper-air westerlies. • Negative 500 hPa gpm anomalies over the subcontinent.
Surface	• Surface pressure trough over the central parts with weaker than normal high pressure to the east. • Negative SLP anomalies in east, positive anomalies in west. • Reduced influx of moisture from the east.	• Surface trough slightly more westward, with high pressure system over the eastern parts. • Positive SLP anomalies in east, negative anomalies in west. • Increased flux of moist Indian ocean air.

Table 4.2. Difference between the mean circulation features in autumn months following the El Niño event of 1982/83 and the La Niña of 1988/89.

MAM	1982/83	1988/89
500 hPa	• The upper-air through west of the subcontinent and a ridge over the central parts of southern Africa. • Positive 500 hPa gpm anomalies over the entire subcontinent. • Increased north-south geopotential gradient, thus increased westerlies.	• More relaxed upper-air slope. • Negative 500 hPa gpm anomalies over the subcontinent. • Reduced north-south geopotential gradient and a weakening in westerlies.
Surface	• Surface pressure through over the western and southern regions which is indicative of enhanced frontal activity over the southern parts. • Surface trough weak and displaced westwards. • Negative SLP anomalies over central, southern and eastern regions, positive anomalies over the northwest.	• Strong east-west pressure gradient which is indicative of westward and southward moisture flux. • Surface trough deeper and over western interior. • Positive SLP anomalies in east, negative anomalies in west.

Taljaard (1989) found that the main cause of the drought and high temperatures during the summer of 1982/83 was the marked increase in westerly wind speed and its greater constancy over the region during December to March. This strong westerlies spread the very dry, subsided air from over the southern Atlantic ocean eastwards and northwards over the land such that the relative humidity and dew points dropped dramatically causing very little cloud and high temperatures. During summer (DJF) the upper-air high pressure system shifts from west (El Niño) to east (La Niña) over the subcontinent. This causes the influx of moist air during warm

events to be from the west, while warmer, moist air is flowing in from the south-east around the upper level anticyclone during cold episodes, enhancing the probability for rainfall over the eastern parts. Geopotential height anomalies during warm event tends to be positive over the subcontinent, while negative anomalies are evident during cold events. This upper level high pressure system is thus stronger developed during warm events. On the surface negative SLP anomalies in the east and positive anomalies in the west occurred during the 1982/83 warm event. The opposite is found during the cold event. The surface high pressure observed in the east is better developed and the surface through tends to be deeper in the case of a cold event than during warm events.

4.5 Summary

It was found in the previous chapter that the interannual changes in the equatorial Pacific Ocean SSTs accounts for large amounts of the total variance of temperature over South Africa. In this chapter the focus was on the interaction between the Pacific Ocean and overlying atmosphere, and subsequently in the effects this coupling has on the circulation over South Africa which leads to anomalous surface temperatures during different phases of ENSO.

By analysing upper-air and surface circulation during the summer and autumn months of the 1982/83 El Niño and the 1988/89 La Niña it was shown that for these cases distinct differences occur that results in different temperature responses over southern Africa. This supports the findings of Taljaard (1989) where he compared the circulation during the La Niña of 1975/76 with the El Niño of 1982/83. As a rule of thumb the upper-air anticyclone is stronger during warm events, enhancing subsidence over the western parts. During a cold event the troughs occur frequently wile stronger anticyclonic circulation over the eastern parts enhance the flux of moist Indian ocean air west- and southwards over the country.

A pressure anomaly dipole exists during both events over the western and eastern parts of South Africa, but it generally changes sign so that positive (negative) SLP anomalies are evident over the western parts and negative (positive) anomalies over the eastern parts during a warm (cold) event.

Although the connection between Pacific Ocean and the atmospheric circulation is described in this chapter, influences from the other oceans surrounding South Africa on the local circulation are also important, especially when the phase of ENSO is not clearly defined in the

Pacific Ocean. Mean conditions in the Atlantic and tropical Indian oceans are vastly different than those in the Pacific mainly owing to its size, position of landmass and absence of El Niño type events (Trenberth, 1991).

A coupling between the ocean and atmosphere exists, causing global scale atmospheric response to the state of the ocean surface. Recent work by van Heerden and Rautenbach (1997) using the CSIRO-9 General Circulation Model with positive SST boundary forcing over the tropical Indian ocean resulted in circulation anomalies similar to those described here. In the next chapter a statistically-based model is constructed to predict seasonal surface-air temperature over South Africa from global scale SSTs.

CHAPTER 5

FORECAST SCHEME

5.1 Introduction

Using singular value decomposition (SVD) it was shown in Chapter 3 that sea-surface temperature can be used as a predictor for seasonal surface-air temperature over South Africa. In this chapter a forecast model is constructed by using the sea-surface temperature predictor field (described in Chapter 2) to predict seasonal mean maximum surface-air temperature (T_x) over South Africa.

5.2 Model Construction

A canonical correlation analysis (CCA) forecast model is constructed to predict seasonal temperature over South Africa. The model is similar to the operational rainfall prediction model used at the South African Weather Bureau (Landman, 1997; Landman and Mason, 1997). The predictor field in the temperature model consists of global scale sea-surface temperature for four consecutive, non-overlapping 3-month periods (for example JFM, AMJ, JAS and OND mean SSTs). By incorporating global scale SSTs at different lags evolutionary SST features, for example the evolution or decaying of an ENSO event which takes place over a number of months, could be included. It was shown by Landman (1997) (predicting rainfall) that model skill could be improved if "stacked" sea-surface temperatures are used. The predictand field consists of mean maximum surface-air temperature for three consecutive months at 77 locations in South Africa (for example mean T_x for March-April-May). Prior to conducting CCA, the standardized predictor and predictand data are separately condensed using empirical orthogonal function (EOF) analysis in order to filter out noise and retain the essential variables. The reduced number of EOF components of the predictor and predictand fields, are then cross-correlated and used as input to the CCA produces. The CCA modes each contain loading patterns for predictors and predictands, a time series for each and a set of eigenvalues which shows the importance of the relationship. Cross-validation is performed to determine the model skill. The predicted values are ranked and divided into three equi-probable categories (or terciles) from which a categorical above-normal, near-normal or below-normal prediction can be made.

Selection of Modes

The optimal number of predictand and predictor modes to describe the data has to be determined. The large number of original modes incorporates a lot of noise that may result in artificial skill (Barnett and Preisendorfer, 1987). On the other hand, limiting the number of predictors and predictands can result in the exclusion of useful information. Therefore a series of cross-validation experiments was performed to seek for the optimal number of modes that would give acceptable forecast skill during all predictand seasons.

Figure 5.1 shows the results of the cross-validated runs for different seasons. For each predictand season the cross-validated skill of SST modes 2 to 7 are plotted against temperature modes 2 to 7. The aim is to identify the optimal model design for all predictand seasons. Four SST modes were found to be responsible for relatively high forecast skill during all seasons and were selected. The sources of skill from global scale SSTs for summer temperature are shown in Figure 5.2. The strongest skill sources during all seasons turned out to be associated with ENSO, a trend in global SSTs and a possible 50 year cycle in sea temperatures (Barnston and Smith, 1996; Landman *et al.*, 1997). By plotting T_x modes against SST mode 4 (Figure 5.3), T_x mode 4 was selected. The strongest modes are associated with ENSO and a seasonal temperature trend (not shown). For the remainder of this study four SST and four T_x modes will be used.

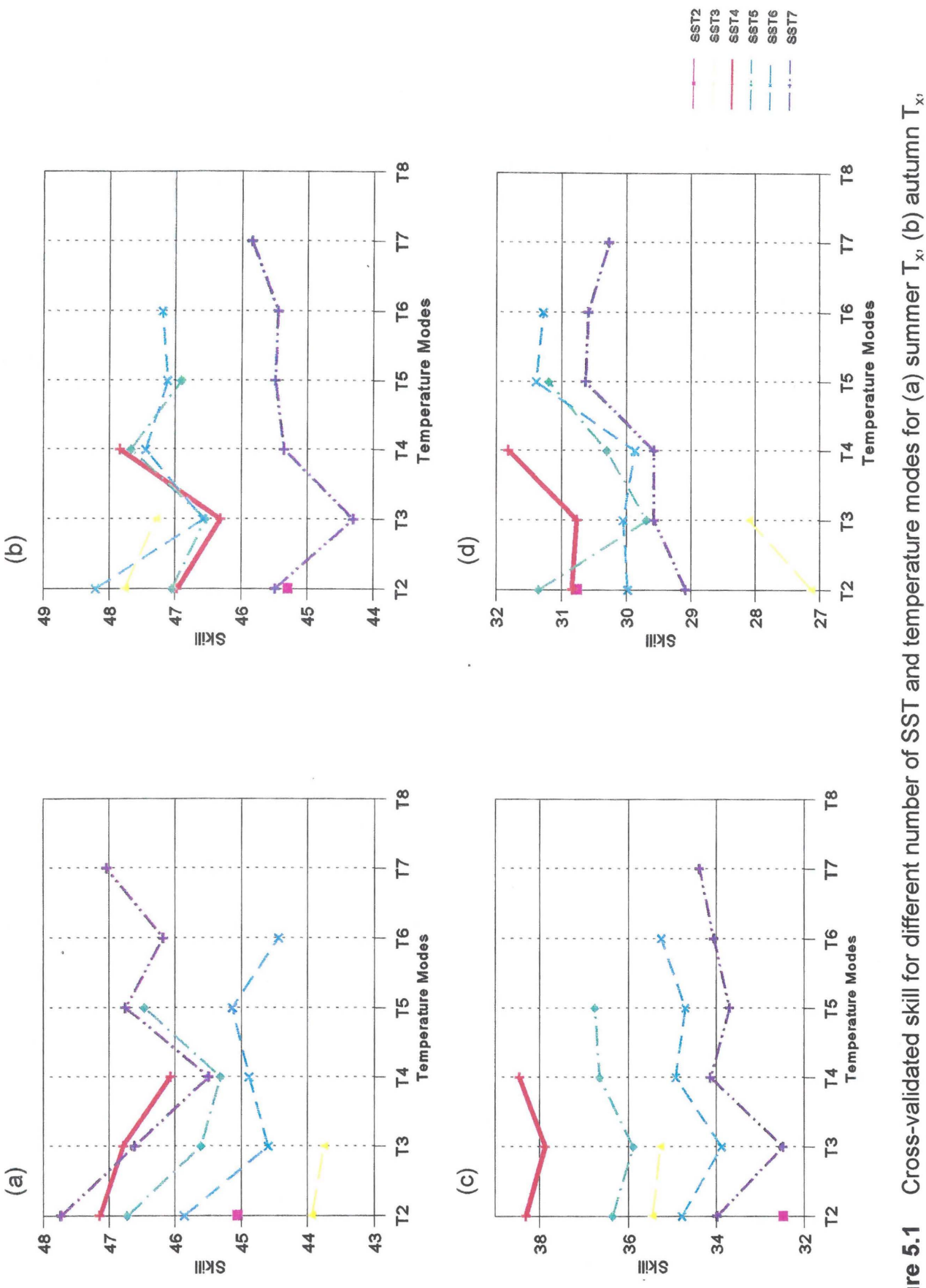

Figure 5.1 Cross-validated skill for different number of SST and temperature modes for (a) summer T_x, (b) autumn T_x, (c) winter T_x and (d) spring T_x.

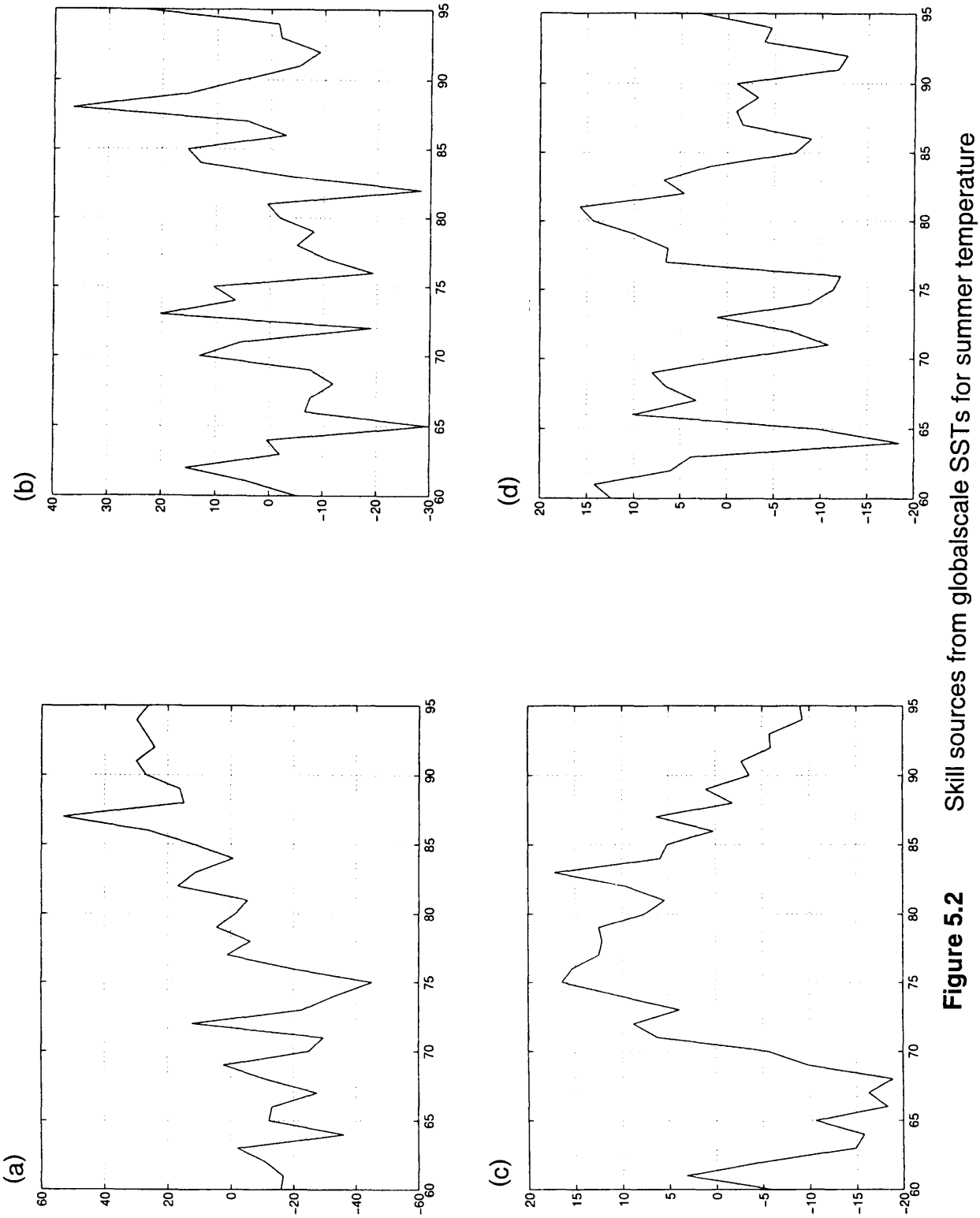

Figure 5.2 Skill sources from globalscale SSTs for summer temperature

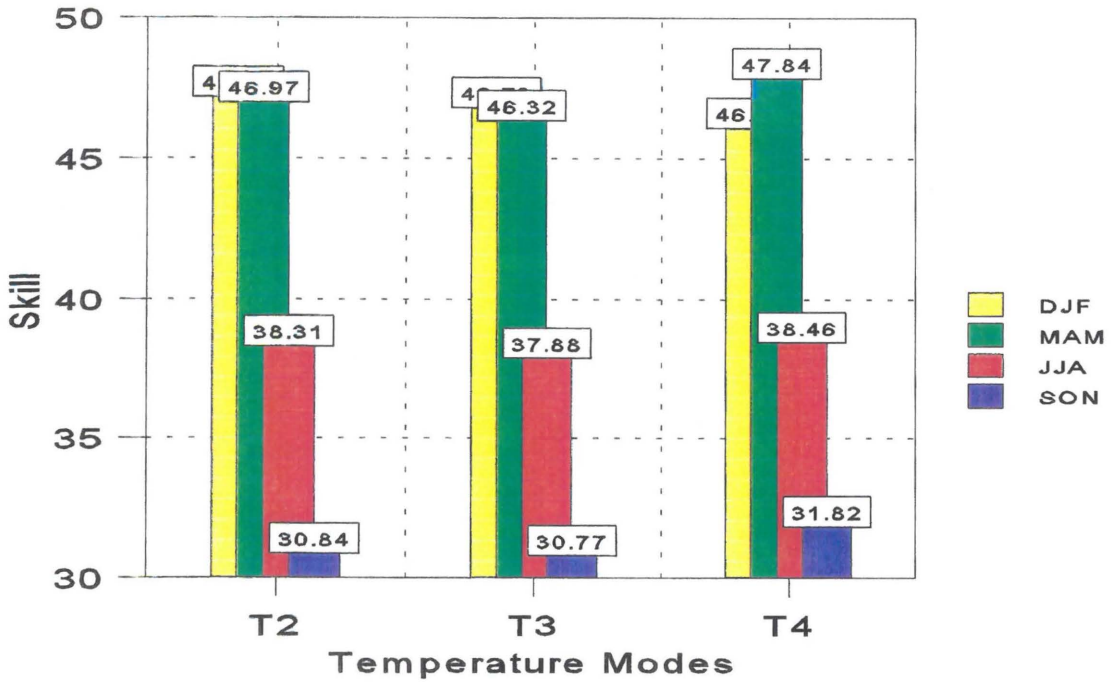

Figure 5.3 Temperature modes T2,T3 and T4 of SST mode 4.

Model Skill

Cross-validation is performed in order to test the skill of the model. An example of a cross-validated run for summer T_x on a 1-season lag is shown in Figure 5.4. In this figure the solid line represents the observed T_x (normalized) for the 36 year training period from 1960/61 to 1995/96, while the dashed line indicates the corresponding predicted indices. Both are averaged over the 77 stations and "AveLocSkill" in the graph is an indication of the average local skill. Mean T_x features associated with the La Niña events of 1973/74 and 1975/76 and the El Niño of 1982/83 are well forecasted. A correlation of 0.56 is found between the predicted and observed values over the 36 year period.

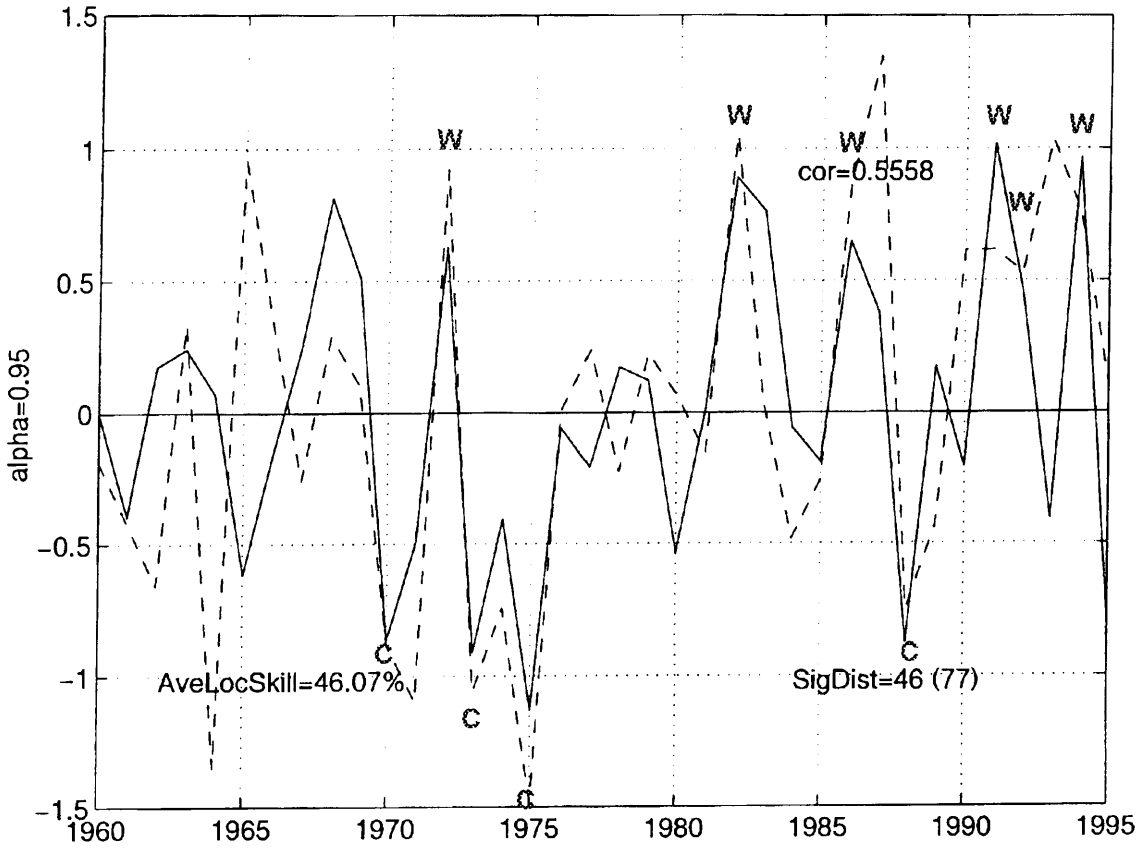

Figure 5.4 Cross-validated prediction for DJF mean maximum seasonal temperature over South Africa. The solid line indicates the mean observed index and the dashed line, the mean predicted index."cor" indicates the correlation between the predicted and observed indices, "AveLocSkill" is the average local skill, "SigDist" indicates the number of stations with significant local skill. "C" and "W" indicate the cold and warm ENSO events.

A number of runs at different lags were performed to test the cross-validated skill of the CCA model for the different seasons. Figure 5.5 shows the results of 1, 2 and 3-season lagged SSTs for the four different temperature seasons. From the figure the skill decreases as the lag increases. JJA is an exception where the skill first decreases and then increases slightly. But still the shortest lag has the highest skill for all four seasons. Also, skill during winter and spring are weaker than during summer and autumn. This is possibly because of the strong teleconnection between equatorial Pacific temperatures and seasonal T_x during summer and autumn that was described in Chapter 3. The previous summer's equatorial Pacific temperatures may not influence spring temperatures as much as it did for autumn because of the longer lag between summer and spring.

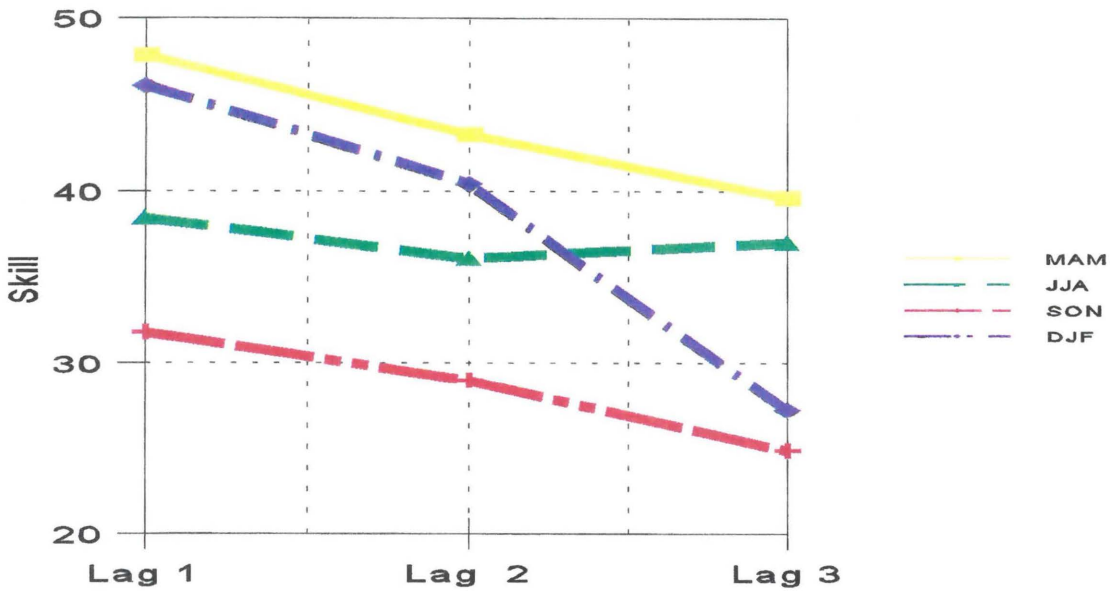

Figure 5.5 1, 2 and 3 season lag skill for the four seasons

Figure 5.6 shows the spatial distribution of significant skill at the 95% level over South Africa for different SST lag periods. The highest skill is found during summer and autumn months and in both cases almost the entire region can be predicted significantly but with short lags. In the case for summer (DJF) the areas with skill above 45% shrink significantly on longer lags. This holds true for autumn as well. During winter (JJA) and spring (SON) months the skill is much lower and confined to the western parts of the country.

5.3 Operational Model

It is now possible to use this CCA temperature model operationally to predict seasonal T_x since the limitations of the model are known. In an operational environment the predictor field will consist of the most recent four 3-month mean stacked SST fields. For example MAM, JJA, SON and $D_{96}JF_{97}$ SSTs are used as predictors for MAM_{97} mean surface-air temperature at 77 stations in South Africa. A categorical forecast for each station is made and stations with significant skill are used to compile a final seasonal forecast. An example of such a forecast is shown for MAM_{97} in Figure 5.7. The A, B or N on the map represents the predicted category, while the number shows the local skill at each station. Skill not significant at the 95% level are indicated with a '-'. Maps like these are compiled for the predicted seasons and an outlook is compiled for each of the nine provinces in South Africa.

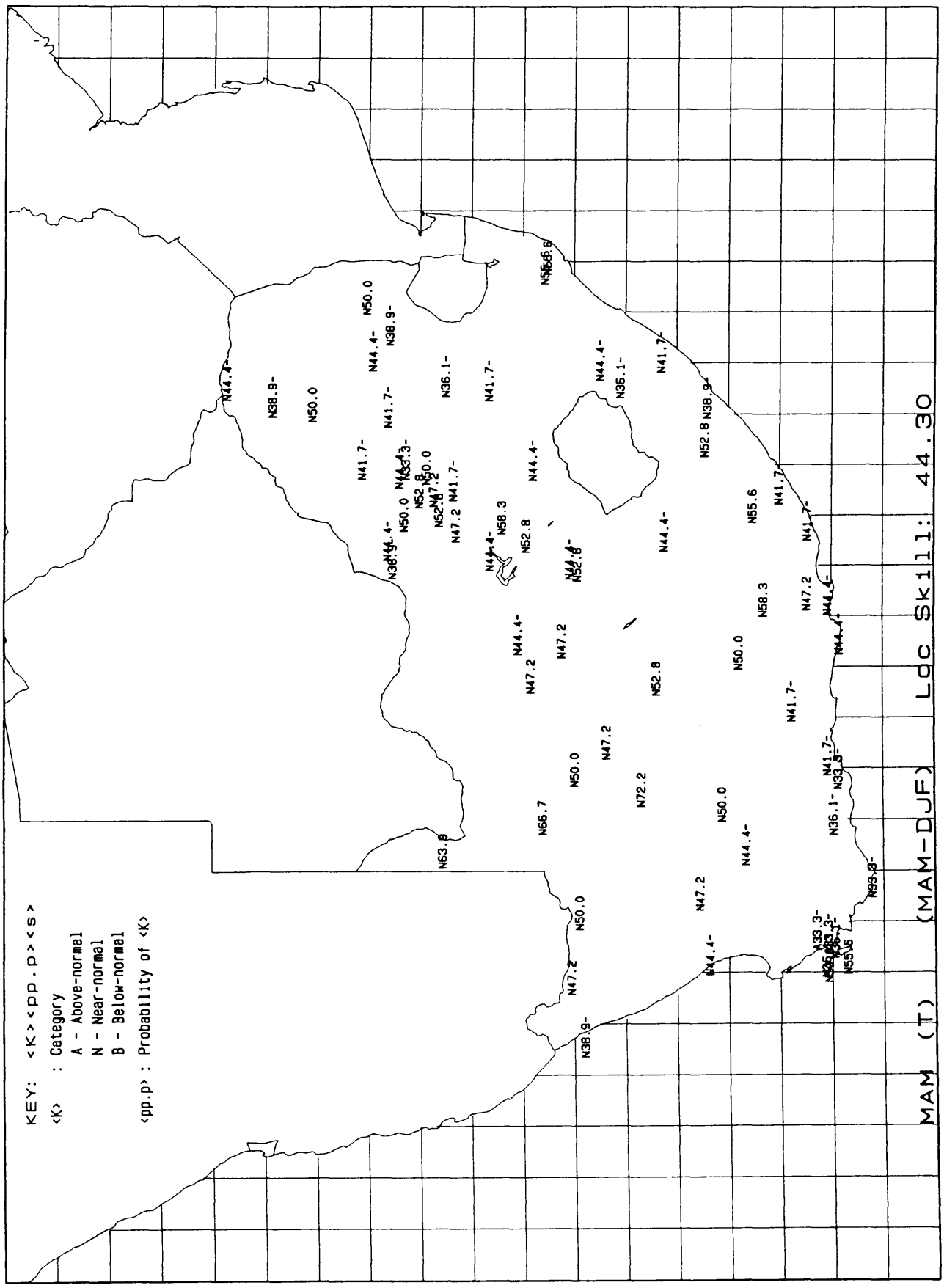

Figure 5.7 Categorical T_x forecats for 77 stations in South Africa for MAM 1997 using MAM_{96} to $D_{96}JF_{97}$ stacked SSTs as predictors. The A, N and B refer to the predicted category. The numbers indicate local skill. The "-" indicates forecasts NOT significant at 95% level.

5.4 Summary

A forecast model is constructed to predict seasonal temperature for a network of 77 stations in South Africa. The statistical method of canonical correlation analysis is used because of its ability to find the optimum linear combination between two data sets. In this case canonical correlation analysis is used to relate principal components of global scale sea-surface temperature to the temperature principal components from 77 stations in South Africa. Firstly the optimal number of predictand (SST) and predictor (T_x) modes that describes the data is determined by performing a number of cross-validated experiments. Four predictor and four predictand modes were found to give optimal skill during all four seasons.

Cross-validation was performed to test the skill of the model at different lagged periods for each season. The shortest lag has the highest skill in all cases. The spatial distribution of significant skill revealed that the highest skill occurs during summer and autumn months, while low cross-validated skill is found for winter and spring. The model described in this chapter has sufficient skill to be used in an operational mode. In the next chapter evaluation of real forecasts is conducted to test the usefulness of such forecasts in an operational environment.

CHAPTER 6

EVALUATION

6.1 Introduction

A forecast model was constructed in the previous chapter to predict seasonal surface-air temperature at different locations in South Africa. Sea-surface temperature of the equatorial Pacific, Indian and southern Atlantic oceans are used as predictors in the forecast scheme. It was also shown in Chapter 3 that ocean temperatures are an important source for seasonal temperature predictability in South Africa, especially during summer and autumn seasons. The proposed forecasts scheme is now evaluated in an operational environment (i.e. over an independent test period) to determine whether such skilful forecasts can be produced successfully.

6.2 Strategy

The assessment of the skill of forecasts is a very difficult matter. Each user of the forecast has a different sensitivity to the product because their use depends on the way the forecasts are presented, the level of detail, and the knowledge of the user to interpret and use the forecast. A forecast evaluation system should be able to test the forecast against observed data in order to provide the user with a measure of the confidence that could be attached to such forecasts.

In order to provide the user with some measure of the value of seasonal temperature forecasts in South Africa, operational model runs were performed for the period from 1987 to 1996. These were then measured against the observed data and the results are presented here. The forecasts of seasonal temperature anomalies for each station are given in terms of three categories, namely below-normal, near-normal or above-normal. The probability of each of these terciles is the same.

A sequence of temperature forecasts was performed for the independant forecast period from 1987 to 1995 for the four climalogical seasons. In each case the climate consists of the 33, 36 or 39 year period (depending on the available data) prior to the forecast season, and the

predictor field consists of four stacked 3-month mean sea-surface temperature for the four seasons prior to the forecast season. Figure 6.1 explains schematically the compilation of data fields for a forecast made for autumn 1987 as an example.

Predictor - Climate	Predictor - Operational	Predictand
$MAMJJASOND_{60}/JF_{61}$ ... $MAMJJASOND_{85}/JF_{86}$	MAM JJA SON D_{86}/JF_{87}	MAM_{87}

Figure 6.1. Presentation of model climate and predictor data set for predicting autumn 1987 seasonal temperature.

Figure 6.2 is an example of a forecast and corresponding observation for March-April-May 1987. This forecast evaluated extremely well and it should be noted that this is not the norm, but the exception. On the plot the capital letters represent the forecast, while the lower case represents the observation. In 71 out of 77 cases the temperature category was predicted correctly. Similar graphs were compiled for all seasons (not shown). Table 6.1 summarizes the number of correct forecasts, one category miss and totally wrong forecasts for the different seasons.

Table 6.1. Summary of hits (out of 77) for each forecast for (a) summer, (b) autumn, (c) winter and (d) spring seasons from 1987 to 1995. The highest score for each case is highlighted.

(a)

Season: DJF	Correct Forecast	Miss 1 category	Miss 2 categories
1987	42	32	3
1988	45	30	2
1989	37	34	6
1990	29	41	7
1991	41	35	1
1992	33	43	1
1993	7	33	37
1994	46	28	3
1995	19	55	3

(b)

Season: MAM	Correct Forecast	Miss 1 category	Miss 2 categories
1987	71	6	0
1988	27	41	9
1989	43	29	5
1990	15	44	18
1991	39	37	1
1992	57	8	12
1993	36	40	1
1994	49	28	0
1995	10	33	34

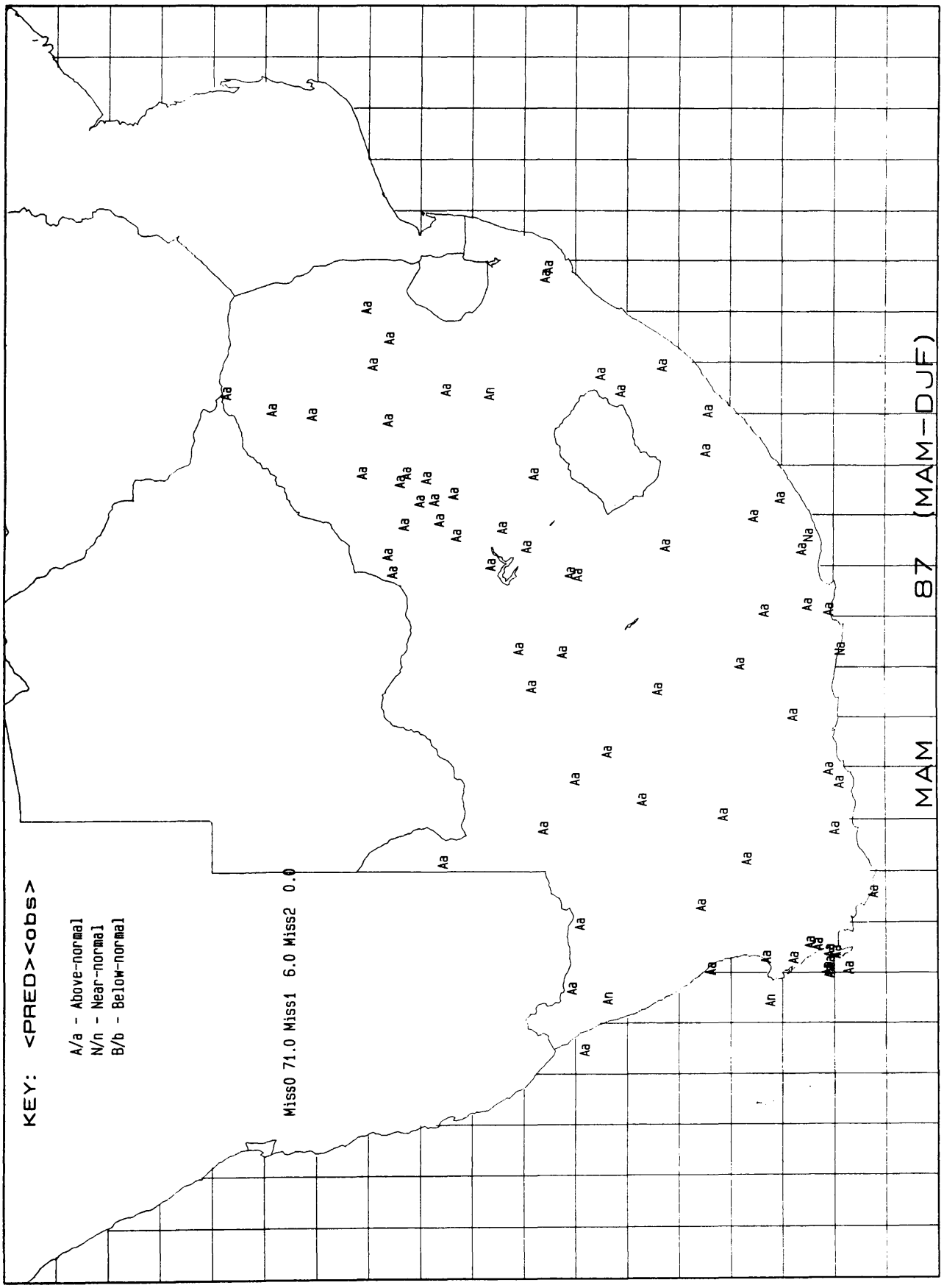

Figure 6.2 Predicted category (A, N, B) and observed category (a, n, b) for MAM 1987 using 0-season lag SSTs.

(c)

Season: JJA	Correct Forecast	Miss 1 category	Miss 2 categories
1987	28	30	19
1988	38	34	5
1989	34	42	1
1990	30	35	12
1991	30	31	16
1992	41	30	6
1993	23	54	0
1994	39	37	1
1995	35	40	2

(d)

Season: SON	Correct Forecast	Miss 1 category	Miss 2 categories
1987	19	43	15
1988	25	49	3
1989	25	41	11
1990	21	45	11
1991	24	38	15
1992	26	44	7
1993	49	27	1
1994	44	31	2
1995	20	51	6

Although Table 6.1 only summarises a simple calculation of the number of hits in each case, a couple of important comments could be made. It is clear that in some years a correct forecast could have been made. And in most cases a forecast for the country as a whole would not be more than one category out. The best forecasts (highest number of hits) occurred for summer and autumn seasons. In the cases of summer 1993 and autumn 1995 wrong forecasts were made, although in both cases the number of hits for 1 category was about equal the number for two categories. By analysing the spatial distribution of forecasts and observations for both cases (summer 1993, autumn 1995) (not shown) above-normal temperatures were predicted for the entire country except the far western and south-western areas. In both cases near-normal to below-normal conditions were observed.

6.3 Evaluation of forecasts

The summary in Table 6.1 only gives an indication of the number of hits for the seasons that are evaluated. The LEPS (linear error in probability space) scores are calculated for each case and presented in Table 6.2. LEPS scoring is described in the literature to be superior to other techniques since the error in terms of the distance between the observed and predicted category is captured. Scores range from -100 to +100. For each season the results for a 0-season lag is presented since the shortest lag was found to have the best skill (Chaper 5).

LEPS skill scores range from -100 to +100% with negative scores indicating the worst possible outcomes (i.e. 2 categories out). From Table 6.2 it is concluded that the LEPS skill of individual evaluated cases varied from episode to episode. Also a variation in skill from season to season is evident. Clearly a higher frequency of skilful forecasts were obtained for summer and autumn, than for the other two seasons. But also the worst predictions were made in summer and autumn (e.g. summer 1993, autumn 1995). The autumn prediction for 1987 evaluated exceptionally well. In this case above-normal conditions were forecasted for the entire country, and it was shown in Figure 6.2 that above-normal seasonal temperatures were observed at all but 6 stations. This resulted in a LEPS skill score of almost 95%. The worst cases resulted in highly negative LEPS scores for autumn 1995 and summer 1993. The poor scores in summer 1993 may have been because of the unexpected El Nino development. The 3-month mean periods predicted for in winter are probably too long to capture events that produce exceptional temperatures.

Table 6.2. LEPS scores calculated for forecasts made for different seasons from 1987 to 1995. Statistically significant values at the 95% level are indicated with an *.

	Summer	**Autumn**	**Winter**	**Spring**
1987	55.21*	94.96*	9.25	-13.66
1988	62.07*	30.44*	41.96*	14.76
1989	17.47	16.02	12.23	-11.37
1990	0.98	-23.73	-1.48	1.95
1991	42.70*	51.69*	-15.38	-7.70
1992	31.57*	58.79*	18.85	1.55
1993	-65.84	43.20*	6.75	51.07*
1994	49.87*	67.92*	9.55	35.90*
1995	8.87	-53.59	6.94	-7.19
Average	22.54	31.74	9.85	7.26

6.4 Summary

Statements about forecast success are not meaningful unless placed in the context of what is expected from such a forecast. In the case of categorical forecasts much of the detail of the distribution of the data are ignored and probabilities are only given in terms of equi-probable terces (or quints in some cases). To evaluate model forecasts made for the period 1987 to 1995 the LEPS score technique was implemented. It was found that during the period the skill varies from season to season, and from year to year. In the mean it is found that forecasts during autumn and summer months were more frequently correct than for winter and spring. It was also seen from a summary of hits and misses during the evaluation period that a totally wrong (2 category miss) seldom occurred, from which it can be said that these forecasts, although not perfect, are better than chance. To asses the usefulness of these predictions in practice it should be tested against the operational use, which is beyond the scope of this dissertation but needs to be addressed.

CHAPTER 7

SUMMARY AND CONCLUSIONS

7.1 Introduction

Until recently seasonal forecasting efforts in South Africa had focused on rainfall. Attempts to provide operational seasonal temperature forecasts to a variety of end users are in the early stages. This study is the first attempt by the South African Weather Bureau to set up a frame work for the prediction of seasonal temperature. Global scale ocean surface temperatures were used to seek for signals that can be related to South African seasonal temperatures. Physical reasons for expecting a link between variations sea-surface temperature and seasonal temperature are that sea-surface temperature anomalies often show strong spatial coherence persisting for several months and can result in large anomalous heat fluxes from the sea to the atmosphere. Therefore the indirect atmospheric response over South Africa to changes in sea-surface temperatures were also investigated.

In the second part of the study the aim was to set up a forecast scheme for seasonal temperature over South Africa that could be implemented operationally. Predicting temperature patterns over areas on seasonal time-scales requires a methodology that is capable of finding pattern-to-pattern (multivariate) relationships, given sets of predictor and predictand elements. In this study an empirical approach was followed to construct a forecast model for seasonal temperatures at 77 locations in South Africa. The model output was verified for a nine year independent period to determine if these predictions are skilful and thus useful in the South African scenario. The results are summarized below.

7.2 Origins of Seasonal Forecast Skill from Global Scale Sea-surface Temperatures

An analysis of the centres of action in the global scale SST field for different seasons reveals two major sources of statistical predictability. ENSO-related features resemble an important influence on the seasonal temperature of South Africa. It was seen that anomalously warm equatorial Pacific ocean surface temperatures coincide with anomalously warm mean seasonal temperatures over South Africa. Also, anomalously cold equatorial Pacific Ocean surface

temperatures coincide with anomalously cold mean seasonal temperatures. This influence from the oceans are mainly evident over the eastern half of the country with the strongest relation with summer and autumn temperatures.

The long-term global warming trend in the equatorial and mid latitude southern oceans capture a large portion of the remaining covariance. It was found that a temperature dipole exists between the northeastern and southwestern areas of South Africa that is usually associated with this warming trend in the oceans. Anomalously cold SSTs in the significant regions will coincide with anomalously warm seasonal temperatures over the southwestern parts and anomalously cold seasonal temperatures over the northeastern parts of South Africa. The opposite tendency is found for anomalous warm SSTs.

It is concluded that:

I) seasonal temperatures over South Africa do respond to variations in global scale sea-surface temperatures;

ii) the strongest skill sources from the oceans are related to ENSO and a global warming trend in the oceans;

iii) there ia a significant response in the temperature field (T_x) to changes in the global scale SSTs during summer and autumn over the eastern half of South Africa.

7.3 Atmospheric Response to Global Scale SST Changes

It is hypothesized that sea-surface temperatures have physical effects on the overlying atmosphere and can modify the large-scale atmospheric circulation. Since a strong ENSO teleconnection signal was found with seasonal temperatures over South Africa, an analysis of the response of mean circulation features over South Africa to the changes in equatorial Pacific SSTs was conducted. It was found that distinct differences in the mean circulation occur between warm and cold ENSO episodes.

i) During warm events the upper-air anticyclone is stronger and positioned more to the west. The westerlies extends westwards over South Africa. During a cold events more throughs occur along the west coast, causing an influx of warm, moist air from the east.

This results in enhanced cloudiness (and rainfall) during cold events, and thus reduced temperatures.

ii) A surface pressure anomaly dipole exists during both cold and warm events between the western and eastern parts of South Africa such that pressure is higher over the western and lower over the eastern parts of the subcontinent during warm events than during cold events.

7.4 Operational Forecasting

A statistically based seasonal prediction scheme has been set up to forecast temperature variability over South Africa. Sea-surface temperatures are employed as the only predictor of seasonal temperature over South Africa.

i) The model that was constructed has sufficient skill to be used in an operational environment. It was found that forecasts which are better than chance can be produced at lead times up to two seasons.

ii) This operational forecast scheme was evaluated over an independent forecasting period from 1987 to 1995. During this period the skill varies from season to season, and from year to year, but a forecast that are two categories out seldom occur.

7.5 Recommendations

i) The forecast model may be improved by incorporating global (all available data) sea-surface temperatures instead of the global scale (440 grid points used in this study) data used in this study. Most importantly more data in the southern Pacific Ocean should be incorporated.

ii) SSTs are used as only predictor for seasonal temperature. Other predictors should be investigated such as persistence and pressure anomalies.

iii) By removing the trend in both data sets the true skill will be obtained.

iv) The statistical relationships shown here are intended as a starting point for the operational prediction of seasonal temperature in South Africa. In the longer-term a

better understanding of the physical relationships will enable more skilful methods to be employed.

v) Non-empirical techniques could be implemented in future to capture the nonlinear relationships between seasonal temperature and certain predictors. These should include dynamical models such as coupled general circulation models.

vi) A perception should be established in the end user community that forecasts are skilful enough to be of value before users of seasonal products may take full advantage of such predictions. Thus, a program of interdiciplanary research is needed to bring the benefits of seasonal predictions to the user.

REFERENCES

AMERICAN METEOROLOGICAL SOCIETY (1983): *Policy Statement of the American Meteorological Society on weather forecasting.* Bull. Amer. Meteor. Soc., Vol. 64, p1385-1387

BARNETT, T.P. (1981): *Statistical Prediction of North American Air Temperatures from Pacific Predictors.* Mon. Wea. Rev., Vol 109, p1021-1041

BARNETT, T.P and R. PREISENDORFER (1987): *Origins and levels of monthly and seasonal forecast skill for United States surface air temperatures determined by Canonical Correlation Analysis.* Monthly Weather Review, Vol 115, p1825-1850

BARNETT, T.P., M. LATIF, E. KIRK and E. ROEKNER (1991): *On ENSO Physics.* J. of Climate, Vol 4, p 487-515

BARNETT, T.P., L. BENGTSSON, K. ARPE, M. FLUGEL, N. GRAHAM, M. LATIF, J. RITCHIE, E. ROEKNER, U. SCHLESE, U. SCHULZWEIDA and M. TYREE (1994): *Forecasting global ENSO- related climate anomalies.* Tellus 46A, Vol 4, p381-397

BARNSTON, A.G. (1992): *Long-lead forecasts of time-mean US surface temperature using canonical correlation analysis.* Proceedings of the 16th Annual Climate Diagnostic Workshop, October 28 to November 1, 1991, Los Angelos, California, p423-429

BARNSTON, A.G. (1994): *Linear statistical short-term climate predictive skill in the Northern Hemisphere.* J. Climate, Vol 7 No 10, p1513-1564

BARNSTON, A.G. and R.E. LIVEZEY (1989): *An operational multifield analog / anti-analog prediction system for United States seasonal temperatures. Part II: Spring, Summer, Fall and Intermediate 3-Month Period Experiments.* J. of Climate, Vol 2, p513- 541

BARNSTON, A.G. and C.F. ROPELEWSKI (1992): *Prediction of ENSO episodes using canonical correlation analysis.* J. Climate, Vol5, p1316-1345

BARNSTON, A.G. and T.M. SMITH (1996): *Specification and prediction of global surface temperature and precipitation from global SST using CCA.* J. of Climate, Vol. 9, p2660-2697

BERLAGE, H.P. (1966): *The Southern Oscillation and World Weather.* Meded. Verh., Vol. 88, 152pp

BJERKNES, J. (1969): *Atmospheric telecionnections from the tropical Pacific.* Mon. Wea. Rev., Vol 97, p103-172

BRETHERTON, C.S., C. SMITH and J.M. WALLACE (1992): *An intercomparison of methods for finding coupled patterns in climate data.* J. Climate, Vol 5, p541-560

CHENG, X. and T.J. DUNKERTON (1995): *Orthogonal rotation of spatial patterns derived from singular value decomposition analysis.* J. of Climate, Vol. 8, No. 11, p2631-2643

CHERVIN, R.M. and T.W. BETTGE (1983): *Response.* Bull. Amer. Meteor. Soc., Vol. 64, p173-1174

CHERVIN, R.M. and T.W. BETTGE (1985): *Response.* Bull. Amer. Meteor. Soc., Vol. 66, p848-849

CHU, P. and Y. HE (1994): *Long-range prediction of Hawain winter rainfall using canonical correlation analysis.* Int. J. Climatol., Vol 14, p659-669

DYMNIKOV, V.P. and S.K. FILIN (1985): *A study of the correlations between sea-surface temperature anomalies in mid-latitudes and anomalies in heating, based on the data from the First GARP Global Experiment.* Reprint of the Dept. Of Numerical Mathematics of the USSR. Academy of Sciences

FOLLAND, C.K., A. WOODCOCK and L. VARAH (1986): *Experimental monthly long-range forecasts for the United Kingdom. Part III. Skill of the monthly forecasts.* Meteor. Mag., Vol. 115, p377-395

FREEMAN, M.H. (1967): *The accuracy of long-range forecasts issued by the Meteorological Office.* Weather, Vol. 22, p72-76

GILL, A.E. (1980): *Some simple solutions for heat induced tropical circulation.* Q.J. Royal Met. Soc., Vol 106, p447-462

GILMAN, D.L. (1985): *Long-range forecasting: The present and the future.* Bul. Am. Met. Soc., Vol 66 No 2, p159-164

GLAHN, H.R. (1968): *Canonical correlation analysis and its relationship to discrimant analysis and multiple regression.* J. Atmos. Sci., Vol 25, p23-31

GLANTZ, M.H., R.W. KATZ and N. NICHOLLS (ed) (1991): *Teleconnections linking worldwide climate anomalies.* Cambridge University Press, 535pp

HALPERT, M.S. and C.F. ROPELEWSKI (1992): *Surface temperature patterns associated with the Southern Oscillation.* J. of Climate, Vol 5, p577-593

HANSEN, J. and S. LEBEDEFF (1987): *Global trends of measured surface air temperature.* J. Geophys. Res., Vol 92, p13345-13372

HARNACK, R.P. (1979): *A further assessment of winter temperature predictions using objective methods.* Mon. Wea. Rev., Vol 107, p250-267

HARNACK, R.P. (1982): *Objective winter temperature forecasts: An update. An extention to the western United States.* Mon. Wea. Rev., Vol. 110, p287-295

HASTENRATH, S (1990a): *Prediction of Northeast Brazil rainfall anomalies.* J. Clim., Vol. 3, p893-904

HASTENRATH, S (1990b): *Tropical climate prediction: A progress report.* Bull. Am. Met. Soc., Vol. 71, p819-825

HEIDKE, P. (1926): *Berechung des Erfolges und der Gute der Windstarkevorhersagen im strumwarnungsdienst.* Geografisika Annaler, Vol. 8, p301-349

HOREL, J.D., V.E. KOUSKY and M.T. KAGANO (1986): *Atmospheric conditions in the Atlantic sector during 1983 and 1984.* Nature, London, Vol 322, p497-509

HOTELLING, H. (1936): *Relations between two sets of variables.* Biometrika, Vol 28, p321-377

JACKSON, J.E. (1991): *A User's Guide to Principal Components.* John Wiley & Sons Inc, New York

JOLLIFFE, I.T. (1990): *Principal component analysis: a beginner's guide - I. Introduction and Application.* Weather, Vol 45, p375-382

JOLLIFFE, I.T. (1993): *Princopal component analysis: A beginner's guide - II. Pitfalls, myths and extensions.* Weather, Vol 48, p246-253

JURY, M.R., B.M.R. PATHACK, C.J.dW. RAUTENBACH and J. VAN HEERDEN (1996): *Drought over South Africa and Indian Ocean SST: Statistical and GCM results.* The Global Atmos. and Ocean System, Vol. 4, p47-63

KATZ, R.W., B.G. BROWN and A.H.MURPHY (1985): *Discision-analystic assesment of the economic value of weather forecasts: The fallowing/planting problem.* J. Forecasting, Vol. 6, p77-89

KILADIS, G.N. and H.F. DIAZ (1989): *Global climatic anomalies associated with extremes in the Southern Oscillation.* J. of Climate, Vol. 2, p1069-1090.

KILADIS, G.N. and H. VAN LOON (1988): *The Southern Oscillation. Part VII: Meteorological Anomalies over the Indian and Pacific Sectors Associated with the extremes of the Southern Oscillation.* Mon. Wea. Rev. Vol 116, p120-136

KNOX, J.B., H. MOSES and M.C. MACCRACKEN (1985): *Summary report of the workshop on the interactions of climate and energy.* Bull. Amer. Meteor. Soc., Vol. 66, p174-183

KOUSKY, V.E., M.T. KAGANO and I.F. CAVALCANT (1984): *A review of the Southern Oscillation: Oceanic-atmospheric circulation changes and related rainfall anomalies.* Tellus, Vol 19, p98-106

LANDMAN, W.A. (1997): *A Study of rainfall variability of South Africa as revealed by multivariate analysis.* Unpublished MSc Dissertation, Univ. of Pretoria

LANDMAN, W.A. and S.J. MASON(1997): *Operational long-lead prediction of South African rainfall, using canonical correlation analysis.* Int. J. Climatol., Submitted

LANDMAN, W.A., dB.D.G. BROOKS and A.G.BARTMAN(1997): *Different modes of evolutionary global-scale sea-surface temperature variability.* Preprints, 5ICSHMO, April 1997, p81-82

LAU, N.C. and M.J. NATH (1994): *A modelling study of the relative roles of tropical and extratropical SST anomalies in the variability of the global atmosphere-ocean system.* J. Clim., Vol 7, p1184-1207

LANZANTE, J.R. (1984): *A rotated eigenanalysis of the correlation between 700-mb heights ans sea surface temperatures in the Pacific and Atlantic.* Mon. Wea. Rev., Vol 112, p2270-2280

LENGOASA, J.R. (1988): *A note on atmospheric circulation and surface temperature fields over South Africa.* SA Geographical J., Vol. 70, no.2, p127-133

LEVEY, K.M. (1993): *Intra-seasonal oscillation of convection over Southern Africa.* Unpublished M.Sc. Dissertation, Univ. Of Cape Town

LIVEZEY, R.E. (1990a): *Variability of skill of long-range forecasts and implications for their use and value.* Bul. Am. Met. Soc., Vol 71 No 3, p300-309

LIVEZEY, R.E. (1990b): *Seasonal predictability and prediction in the extra-tropics.* WMO: Programme on Long-range Forecasting Research Report No. 13, WMO, p15-19

LIVEZEY, R.E. (1995): *The evaluation of forecasts.* Analysis of Climate Variability. Applications of statistical techniques. H. von Storch and a. Navarra (Eds), Spinger-Verslag, Berlin, Chapter 10, p177-196

LIVEZEY, R.E. and A.G. BARNSTON (1988): *An operatonal multi-field analogue/anti-analogue prediction system for United States seasonal temperatures. Part 1: System design and winter experiments.* J.Geophys. Res., Vol. 93, p10953-10974

MADDEN, R.A. (1977): *Estimates of autocorrelations and spectra of seasonal mean temperatures over North America*. Mon. Wea. Rev., Vol 105, p9-18

MASON, S.J. (1992): *Sea surface temperature and South African rainfall variability.* Unpublished Ph.D Thesis, Univ. of the Witwatersrand, Johannesburg

MASON, S.J., A.M. JOUBERT, C. COSIJN and S.J. CRIMP (1996): *Review of seasonal forecasting techniques and their applicability to Southern Africa.* Water SA, Vol 22, No 3, p203-209

MICHAELSEN, J. (1987): *Cross-validation in statistical climate forecast models.* J. Climate Appl. Meteor., Vol 26, p1589-1600

MüHLENBRUCH-TEGEN, A (1992): *Long-term surface temperature variations in South Africa.* SA Tydskrif vir Wetenskap, Vol. 88, p197-205

NEWELL, R.E. and B.C. WEARE (1976): *Factors governing tropospheric mean temperature.* Nature, Vol. 194, p1413-1414

NICHOLLS, N. (1987): *The use of canonical correlation to study teleconnections.* Mon. Wea. Rev., Vol 115, p393-399

OLIVER, J.E and J.J. HIDORE (1984): *Climatology.* New York, Charles E. Merril Publishing Company, 1984, 380pp

PALMER, T.N. and L.T. ANDERSON (1994): *The prospects for seasonal forecasting.* Q.J. Royal Meteorol. Soc., Vol 120, p755-793

PAN, Y.H. and A.H. OORT (1990): *Correlation analysis between sea surface temperature anomalies in the eastern equatorial Pacific and the world ocean.* Climate Dyn., Vol 4, p191-205

PEIXOTO, J.P. and A.H. OORT (1992): *Physics of Climate.* Amer. Institude of Physics

PHILANDER, S.G. (1990): *El Niño, La Niña, and the Southern Oscillation.* Academic Press Inc, London, 293pp

POTTS, J.M., C.K. FOLLAND, I.T. JOLLIFFE and D. SEXTON (1996): *Revised "LEPS" scores for assessing climate model simulations and long-range forecasts.* J. of Climate, Vol. 9, p34-53

PREISENDORFER, R.W. (1988): *Principal Component Analysis in Meteorology and Oceanography.* Elsevier, New York

PREISENDORFER, R.W., F.W. ZWIERS and T.P. BARNETT (1981): *Foundations of Principal Component Selection Rules.* SIO Reference Series 81-4, Scripps Institude of Oceanography, La Lolla, CA

PREISENDORFER, R.W. and C.D. MOBLEY (1984): *Climate forecast verifications, United States Mainland,1974-83.*Mon. Wea. Rev., Vol 112, p809-825

PREISENDORFER, R.W., C.D. MOBLEY and T.P. BARNETT (1988): *The principal disriminant method of prediction: Theory and Evaluation.* J. Geophys. Res., Vol 93, p10815-10830

PROHASKA, J. (1976): *A technique for analysing the linear relationships between two meteorological fields.* Mon. Wea. Rev., Vol 104, p1345-1353

RASMUSSON, E.M and T.H. CARPENTER (1982): *Variations in tropical sea surface temperature and surface wind fields associated with the Southern Oscillation / El Niño.* Mon.Wea. Rev. Vol 110, p354-384

RASMUSSON, E.M. and J.M. WALLACE (1983): *Meteorological aspects of the El Niño / Southern Oscillation.* Science, Vol 222, p1195-1202

RAUTENBACH, C.J.dW. (1997): *A GCM study describing teleconnections between global SST anomalies and the copious summer rainfall over Southern Africa (1995/96).* Preprints, 5ICSHMO, April 1997, p1-2

RENWICK, J.A. and J.M. WALLACE (1995): *Predictable anomaly patterns and the forecast skill of Northern Hemisphere wintertime 500 mb height fields.* Mon. Wea. Rev., Vol 123, p2114-2131

REYNOLDS, R.W. (1988): *A real-time global sea-surface temperature analysis.* J. Clim., Vol 1, p75-86

REYNOLDS, R.W. and D.C. MARSICO (1993): *An improved real-time global sea-surface temperature analysis.* J. Climate, Vol 1, p75-86

REYNOLDS, R.W. and T.M. SMITH (1994): *Improved global sea surface temperature analysis using optinum interpolation.* J. Clim., Vol 7, p929-948

RICHMAN, M.B. (1986): *Rotation of Principal Components.* J. Climatol., Vol 6, p293-335

ROPELEWSKI, C.F. and M.S. HALPERT (1987): *Global and regional scale precipitation patterns associated with the high index phase of El Niño / Southern Oscillation.* Mon. Wea. Rev., Vol. 115, p3078-3096

ROPELEWSKI, C.F. and M.S. HALPERT (1989): *Precipitation patterns associated with the high index phase of the Southern Oscillation.* J. Climate, Vol. 2, p268-284

RUSMUSSON, E.M. and T.H. CARPENTER (1982): *Variation in tropical sea surface temperature and surface wind fields associated with the Southern Oscillation/El Niño.* Mon. Wea. Rev., Vol 110, p354-384

SCHULZE, B.R. (1965): *Climate of South Africa - Part 8: General Survey.* WB 28, Republic of South Africa, 330pp

SCHULZE, G.S. (1989): *Seisoensvariasies van reënval oor die somerreënstreke van Suid-Afrika.* Unpublished MSc dissertation, 205pp

SHUKLA, J. and D.A. PAOLINI (1983): *The Southern Oscillation and longe-range forecasting of the summer monsoon rainfall over India.* Mon. Wea. Rev., Vol 111, p1830-1837

SNEYERS, R. and C. GOOSSENS (1987): *The Principal Component Analysis. Application to climatology and to meteorology.* WMO 9th session of CCI. Report of the rapporteur on statistical methods. Annex. Final version, 51pp

SONKA, S.T., S.A. CHAGNON and S. HOFING (1988): *Assesing climate information use in agri-business. Part 1: Actual and potential use and impediments to usage.* J. Climate, Vol. 1, p757-765

STONE, M. (1974): *Cross validatory choice and assessments of physical predictions.* J. Roy. Stat. Soc., Vol B36, p111-147

TALJAARD, J.J. (1989): *Climate and circulation anomalies in the South African region during the dry summer of 1982/83.* Technical Note No. 21, South African Weather Bureau, 45 pp

TALJAARD, J.J. (1996): *Atmospheric circulation systems, synoptic climatology and weather phenomena of South Africa. Part 5: Temperature phenomena in South Africa.* Technical Note No. 31, South African Weather Bureau

TATSUOKA, M. (1988): *Multivariate analysis.* Macmillan, New York, p241-249

TENNANT, W.J. (1997): *Monthly forecasting in South Africa.* Preprints, 5ICSHMO, April 1997, p154-155

THIAO, W. and A.G. BARNSTON (1997): *Long-lead predictability of summer rainfall in southern Africa.* Preprints, 5ICSHMO, April 1997, p156-157

TRENBERTH, K.E. (1991): *General Characteristics of El Niño-Southern Oscillation.* Teleconnections linking worldwide climate anomalies, Chapter 2, University Press, Cambridge, p13-42

TRENBERTH, K.E. and D.J. SHEA (1987): *On the evolution of the Southern Oscillation.* Mon. Wea. Rev., Vol 115, p3078-3096

TYSON, P.D. (1986): *Climate change and variability in Southern Africa.* Oxford Univ. Press, Cape Town

VAN HEERDEN, J. and C.J.dW. RAUTENBACH (1997): *A GCM simulation of the impact on the atmospheric circulation over Africa by boundary forcing due to sea surface temperature anomalies in the central Indian Ocean.* Preprints, 5ICSHMO, April 1997, p196-197

VAN LOON, H. and R.A. MADDEN (1981): *The Southern Oscillation. Part 1: Global associations with pressure and temperature in northern winter.* Mon. Wea. Rev., Vol 109, p1150-1162

WALKER, G.T. (1923): *Correlation is seasonal variations of weather. VIII. A prelimanary study of world weather.* Mem. Indian Meteor. Dep., Vol 24, No 4, p75-131

WALKER, G.T. (1924): *Correlation is seasonal variations of weather. IX. A further study of world weather.* Mem. Indian Meteor. Dep., Vol 24, No 9, p275-332

WALKER, G.T. (1928): *World weather. III.* Mem. R. Meteor. Soc., Vol 2, p97-106

WALKER, G.T. and E.W. BLISS (1932): *World Weather IV.* Mem. Roy. Meteor. Soc., Vol. 3, p81-95

WALKER, G.T. and E.W. BLISS (1932): *World Weather V.* Mem. Roy. Meteor. Soc., Vol. 4, p53-84

WALKER, G.T. and E.W. BLISS (1937): *World Weather VI.* Mem. Roy. Meteor. Soc., Vol. 4, p119-139

WARD, M.N. and C.K. FOLLAND (1991): *Prediction of seasonal rainfall in the north Nordeate of Brazil using eigenvectors of sea-surface temperature.* Int. J. Climatol., Vol. 11, p711-743

WMO (1994): *Climate variability, agriculture and forestry.* Technical Note 196, WMO No. 802